# Application of deep dehumidification technology in low-humidity industry: A review

Review article

# Application of deep dehumidification technology in low-humidity industry: A state-of-the-art review

Qunli Zhang [a,b,*], Yanxin Li [a], Qiuyue Zhang [a], Fengge Ma [a], Xiaoshu Lü [b,c,d]

[a] Beijing Municipality Key Lab of Heating, Gas Supply, Ventilation and Air Conditioning Engineering, Beijing University of Civil Engineering and Architecture, Beijing 100044, China

[b] Collaborative Innovation Center of Energy Conservation & Emission Reduction and Sustainable Urban-Rural Development in Beijing, Beijing 100044, China

[c] Department of Electrical Engineering and Energy Technology, University of Vaasa, P.O.Box 700, FIN-65101, Vaasa, Finland

[d] Department of Civil Engineering, Aalto University, P.O.Box 12100, FIN-02130, Espoo, Finland

## Abstract

Humidity regulation plays a pivotal role in both residential and industrial environments, significantly impacting comfort, health, and process efficiency. The integration of dehumidification systems with air conditioning systems allows for the control of temperature and humidity, resulting in a decrease in carbon dioxide emissions. In order to address the demands of industries with low humidity levels, this study offers a comprehensive review of advanced deep dehumidification systems. The study initially delineates the specific ranges for deep dehumidification as outlined in academic research, as well as the humidity levels in low-humidity industries. Evaluation models are proposed for the analysis of the dehumidification performance, energy efficiency, economic feasibility, and environmental impact of the system. The review focuses on the deep dehumidification technology, which encompasses air compression dehumidification, liquid desiccant dehumidification, solid desiccant dehumidification, membrane dehumidification, and coupled dehumidification, with an emphasis on materials, components, and systems flow. The research provides a comprehensive overview of the various potential applications of dehumidification systems, including air humidification, water collection, air purification, intelligent control, and optimization. Moreover, a comprehensive comparative analysis of different dehumidification technologies is conducted with regard to industrial application humidity requirements, energy performance, economic factors, and environmental considerations. Drawing on advanced studies and findings, this research examines the primary areas for future development in

* Corresponding author. Qunli Zhang, doctor, professor. Tel: +861068322517.
E-mail address: zhangqunli@bucea.edu.cn

advancing deep dehumidification systems. The objective of this study is to propose optimization techniques aimed at enhancing dehumidification efficiency and reducing energy consumption in low-humidity industrial settings.

**Highlights**

- Summarise desiccant, component, and system aspects of deep dehumidification technology
- Provide recommendations for optimizing methods of the dehumidification efficiency and energy efficiency
- Suggest dehumidification systems applications in industries with different humidity ranges
- Analyse energy, economic, and environmental aspects of dehumidification systems
- Discuss main future works for deep dehumidification systems

**Keywords:** Deep humidification; Desiccant; Air humidity; Dew point temperature; Energy consumption

Review

**Nomenclature**

| Abbreviations | | Symbols | |
|---|---|---|---|
| *PPMV* | Parts Per Million Volume | $R_d$ | Dehumidification rate (moisture removal capacity), kg/s |
| PPM | Parts per million | $M_p$ | Flow rate of process air, kg/s |
| *DEG* | Diethylene glycol | $d_{p,in}$ | Process air humidity of inlet, kg/s |
| EG | Ethylene glycol | $d_{p,out}$ | Process air humidity of outlet, kg/s |
| *TEG* | Triethylene glycol | $d_{equ,in}$ | Air absolute humidity in equilibrium with the inlet solution at its temperature and concentration, g/kg |
| LiCl | Lithium chloride | $\eta_d$ | Dehumidification efficiency (effectiveness) |
| *LiBr* | Lithium bromide | $COP_t$ | The coefficient of performance of the total dehumidification system |
| $CaCl_2$ | Calcium chloride | $Q_t$ | The total heat exchange of process, kW |
| *KCOOH* | Potassium Formate | $W_t$ | The total system energy consumption by heating, cooling, and dehumidification, kW |
| $CH_3COOK$ | Potassium acetate | i | The gas to be tested, consisting process air and regeneration air |
| $CH_3COONa$ | Sodium acetate | $C_p$ | The specific heat capacity, kJ/(kg·K) |
| $HCO_2K$ | Potassium formate | $W_{latent}$ | The energy consumption of latent heat, kW |
| *PG* | Propylene glycol | $R_e$ | The water removal value of per unit electricity, kJ/g |

| | | | |
|---|---|---|---|
| [Dmin]OAC | 1,3-dimethylimidazolium acetate | $C_e$ | The electricity power consumption, kW |
| *[Emin]BF4* | 1-Ethyl−3-methylimidazolium Tetrafluoroborate | *d* | Humidity ratio, g/kg |
| *[Emin]OAC* | 1-Ethyl-3-methylimidazolium | $A_{ratio}$ | The area ratio of desiccant wheel |
| PVP | Polyvinylpyrrolidone | $A_p$ | The area of process air, $m^2$ |
| *$TiO_2$* | Titanium dioxide | $A_r$ | The area of regeneration air, $m^2$ |
| *MOFs* | Metal organic Framework | $COP_{latent}$ | The coefficient of latent heat performance of the dehumidification system |
| PVA | Polyvinyl alcohol | $P_P$ | Payback period, year |
| PEI | Polyetherimide | I | initial investment, $ |
| PAN | Polyacrylonitrile | $p_e$ | Electricity price, $/kWh |
| PDMS | Polyacrydimethylsiloxane | x | conventional energy |
| PES | Poly(ether sulfone) | $C_x$ | Conventional energy consumption |
| SPEEK | Sulfonated poly (ether ketone) | $p_x$ | Conventional energy price |
| NTU | Number of transfer unit | $m_{CO_2}$ | $CO_2$ emissions, kg |
| RH | Relative humidity | $EF_e$ | Carbon emission factor of electricity, $kgCO_2/kWh$ |
| $CO_2$ | Carbon dioxide | $EF_x$ | Carbon emission factor of conventional energy |
| HVAC | Heating, ventilation, and air conditioning | $d_{surface}$ | Air humidity ratio of the saturated air layer on the surface of the solution, g/kg |
| COP | Coefficient of performance | *Rd* | Dehumidification rate (moisture removal capacity), kg/s |
| | | *Mp* | Flow rate of process air, kg/s |
| | | *Pv* | Water vapor partial pressure of the saturated air layer on the surface of the solution, kPa |
| | | *P* | System operation pressure, kPa |

## 1. Introduction

Paris Agreement, which aims to restrict global climate warming to 1.5 °C, signifies a crucial commitment. The presence of hot and humid air is a contributing factor to the increased energy demand for operating heating, ventilation, and air conditioning (HVAC) systems, which accounts for approximately 20%–40 % of the total energy consumption in buildings [1]. The greenhouse gas emissions from sensible load amount to 599 Mt $CO_2$, constituting 31 % of total

air conditioning emissions and 53 % of cooling energy emissions [2]. Meanwhile, humidity serves as a crucial indicator in both building and industrial settings, as it plays a significant role in maintaining thermal comfort, physical well-being, and industrial productivity. According to ASHRAE Standard 55–2017, the maximum allowable air humidity ratio in a HVAC system is 12.0 g/kg (within the dry bulb temperature range of 20 °C–28 °C). Low-humidity requirements in industrial applications, including production, transportation, and storage, are detailed in Table 1. The design and selection of dehumidification systems are of particular significance in light of the rapid expansion of global industrialization and construction, taking into account factors such as dehumidification performance and energy consumption.

Table 1. Summary of humidity requirements in low-humidity industry.

| Industry | Specific scenarios | Air humidity ratio | Air dew point temperature | Reference |
|---|---|---|---|---|
| Lithium battery | Coating and rolling slitting | 0.35–3.47 g/kg | −26.13 to −1.01 °C | [3] |
| | Drying and electroy | 15 ppmv | −60 to −35 °C | [4] |
| | Formation | 0.01–0.23 g/kg | −60 to −30 °C | [3] |
| Food | Meat processing | 2.27–4.56 g/kg | −6.02–2.6 °C | |
| | Brewery production | 2.27–3.03 g/kg | −6.02–2.63 °C | |
| | Chocolate storage | 0.31–1.38 g/kg | −27.24–11.61 °C | [5] |
| Chemical | Natural gas production and dehydration | 143 ppmv | −40 °C | [6] |
| Medical | Effervescent tablets | 2.03–3.40 g/kg | −7.28 to −1.27 °C | [3] |
| | Soft capsules | 2.74–5.56 g/kg | −3.8 to −5.4 °C | |
| | Medical Device Gas | 0.04 g/kg | −45 °C | [7] |
| Storage | Low temperature cold storage | 0.63 g/kg | −20 °C | [8] |
| | Film library and audio-visual library | 3.47–4.51 g/kg | −1.02 to −2.46 °C | [3] |
| | Seed warehouse | 1.34–2.68 g/kg | −11.95 to −4.09 °C | |

Conventional air conditioning systems are designed to manage both the latent and sensible loads of chilled water (7°C–12 °C) or refrigerant. The optimal dew point temperature can be reached

as low as 5 °C using chilled water at 7 °C. When the surface temperature of the cooling coil falls below 0 °C, water vapor condenses and freezes on the coil's surface, leading to a decrease in cooling efficiency and the dehumidification effect. A dehumidification-hybrid air conditioning system is characterized as a control system that is independent of temperature and humidity, and it manages the latent load through the dehumidifier and the sensible load through the cooling unit. By elevating the temperature of chilled water and substituting R134a refrigerants with LiCl solutions, the dehumidification-hybrid air conditioning system achieves a reduction in carbon dioxide emissions. The dehumidification-hybrid air conditioning system is capable of attaining a dew point temperature of 0 °C.

Dehumidification has garnered considerable attention in the last five years, as illustrated in Fig. 1. A search on the Web of Science using the keyword "dehumidification" yielded a total of 2335 articles published between 2017 and 2023, with the annual number of publications showing a consistent increase (except for 2023). Two-thirds of the publications are attributed to developing countries, with China and India contributing 41.12 % and 10.36 % of the total, respectively. This discovery indicates that dehumidification systems have significant potential for growth in developing nations. Following a more rigorous screening process that excluded articles related to desalination and those that did not comply with the criteria, only 61 review articles related to dehumidification were identified. Out of all the review articles, only 11.5 % have comprehensively examined the materials, components, and systems. Consequently, the most recent and widely referenced articles on various dehumidification technologies were chosen for analysis. As indicated in Table 2, numerous review studies have undertaken a thorough examination of the contemporary dehumidification systems. In the literature review, all the studies thus far have demonstrated that a dehumidification-hybrid air conditioning system can achieve dehumidification at a lower dew point temperature. However, due to the intricate characteristics of dehumidification systems, a comprehensive summary of the impacts of dehumidification capacity, energy, economy, environment, and dehumidifier design has not yet been achieved. Consequently, it is imperative to address the following areas of knowledge deficiency.

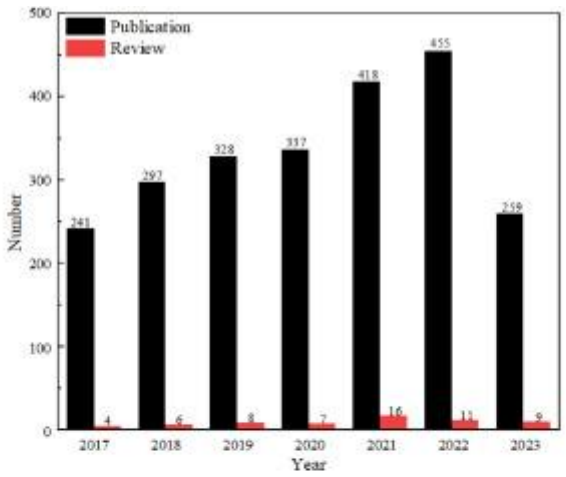


(a) Trends in dehumidification research publications.

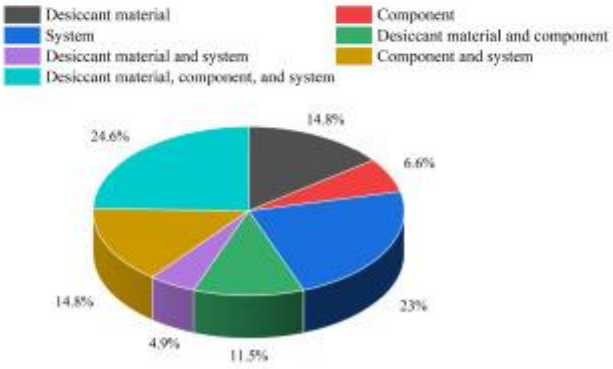


(b) Different research themes in dehumidification literature review.

Fig. 1. Summary of dehumidification publications from 2017 to 2023 (Web of Science).

Table 2. Critical analysis of dehumidification technologies in recent literature reviews.

| Dehumidification technology | Review content | Gap | Publish year | Reference |
|---|---|---|---|---|
| Solid desiccant dehumidifiers | Desiccant materials properties, dehumidifiers, regenerators, dehumidification performance, and energy consumption | Absence in comparative analysis of different materials and systems, limited application scenarios to building | 2020 | [9] |
| Solar powered solid desiccant-vapor compression hybrid cooling system | Modeling and effects of system performance parameters | Absence in impact of solar energy regeneration on dehumidification performance, without detailed consideration of investment payback period | 2018 | [10] |

| Dehumidification technology | Review content | Gap | Publish year | Reference |
|---|---|---|---|---|
| Desiccant air-conditioning systems | System configurations, operating processes, and performance indicators<br>Design and control optimizations of system | Absence in optimized design for desiccants and dehumidification components | 2021 | [11] |
| Solid desiccant-based dehumidification systems | Configurations, techniques, and current trends of system | Absence in evaluation models for solid desiccant dehumidification system | 2022 | [12] |
| Liquid desiccant dehumidification system | Correlations and enhancement approaches for heat and mass transfer of system | Absence in optimization researches on system configurations | 2019 | [13] |
| Liquid desiccant air dehumidification | Materials, components, systems and optimization methods | Absence in practical engineering application researches | 2020 | [14] |
| Membrane-based air dehumidification | Membrane characteristics, membrane configurations, membrane-related mass transport mechanism, system design and operation, and the mass transfer modeling | Absence in research progress beyond membrane materials | 2018 | [15] |

The dehumidification capacities of various technologies differ, and this study introduces the concept of deep dehumidification. Deep dehumidification is characterized by the adherence to strict outlet humidity thresholds. While various disciplines have contributed to the definition of these ranges, the primary emphasis has been on parameters such as humidity ratio, dew point temperature, and relative humidity. A thorough examination of these profound dehumidification definitions, as outlined in Table 3, demonstrates significant variation among the studies. Absolute humidity is a parameter that precisely represents the amount of water vapor present in a specific volume of air. The relative humidity frequently fluctuates in response to changes in environmental temperature, and there is a direct correlation between the logarithm of the air dew point temperature and the humidity ratio in the air [16]. The majority of studies have defined the deep dehumidification range as being below 6 g/kg. This is due to the fact that

the use of chilled water at 7.0 °C can efficiently control indoor humidity levels to as low as 6 g/kg. It would be difficult to decrease the air humidity ratio below this value, given the necessary humidity difference of 2.0–5.0 g/kg for mass transfer [17]. Given the varied interpretations of deep dehumidification across different disciplines, this study establishes deep dehumidification as the condition in which the supply air possesses a humidity ratio below 6 g/kg or an air dew point temperature of 5 °C.

Table 3. Summary of research on different deep dehumidification ranges.

| Deep dehumidification ranges | System description | Reference |
|---|---|---|
| Dehumidify the air from 19.26 g/kg to 7.53 g/kg | LiCl–$H_2O$ solution | [18] |
| Air humidity below 7 g/kg | No requirements | [19] |
| Dehumidify the air from 19 g/kg to 6.8 g/kg | LiCl–$H_2O$ solution | [20] |
| Air humidity below 6.2 g/kg | No requirements | [21] |
| Air humidity below 6 g/kg | Silica gel desiccant wheel | [22] |
| Air humidity below 5 g/kg | No requirements | [[23], [24], [25]] |
| Dehumidify the air from 19 g/kg–14 g/kg to 4 g/kg | Two-stage desiccant wheel | [26] |
| Air dew point temperature: −20°C to −65 °C | No requirements | [27] |
| Air relative humidity below 60 % | Cooling and solid desiccant | [28] |

Different from previous review efforts, this study is structured in a manner that systematically addresses the following concerns.

(1) The proposal outlines the concept of deep dehumidification, emphasizing experimental and simulation research on materials, components, and systems.
(2) This research analyzes the significant advancements made by various methods in enhancing dehumidification performance and decreasing energy consumption in systems in recent years. The objective is to design multifunctional systems for future applications.
(3) This study examines the structural dimensions, dehumidification performance, energy performance, economic aspects, and environmental impact of various dehumidification systems in practical applications. Design recommendations for appropriate solutions in various areas with dehumidification needs are also introduced.

The substantial body of work serves as the basis for conducting quantitative analysis and making recommendations to further investigate the development of the deep dehumidification

system. The technical overview of this review study is depicted in Fig. 2. The evaluation models for dehumidification systems are established in Section 2. The advanced method for reviewing and improving desiccant materials, components, and systems is summarized in Section 3. The multifunctional development of dehumidification systems is primarily elucidated in Section 4. Subsequently, Section 5 examines the dehumidification, energy, economic, and environmental performance of various dehumidification systems. The aim of this study is to provide valuable insights and recommendations for future use by researchers and practitioners working in low-humidity environments.

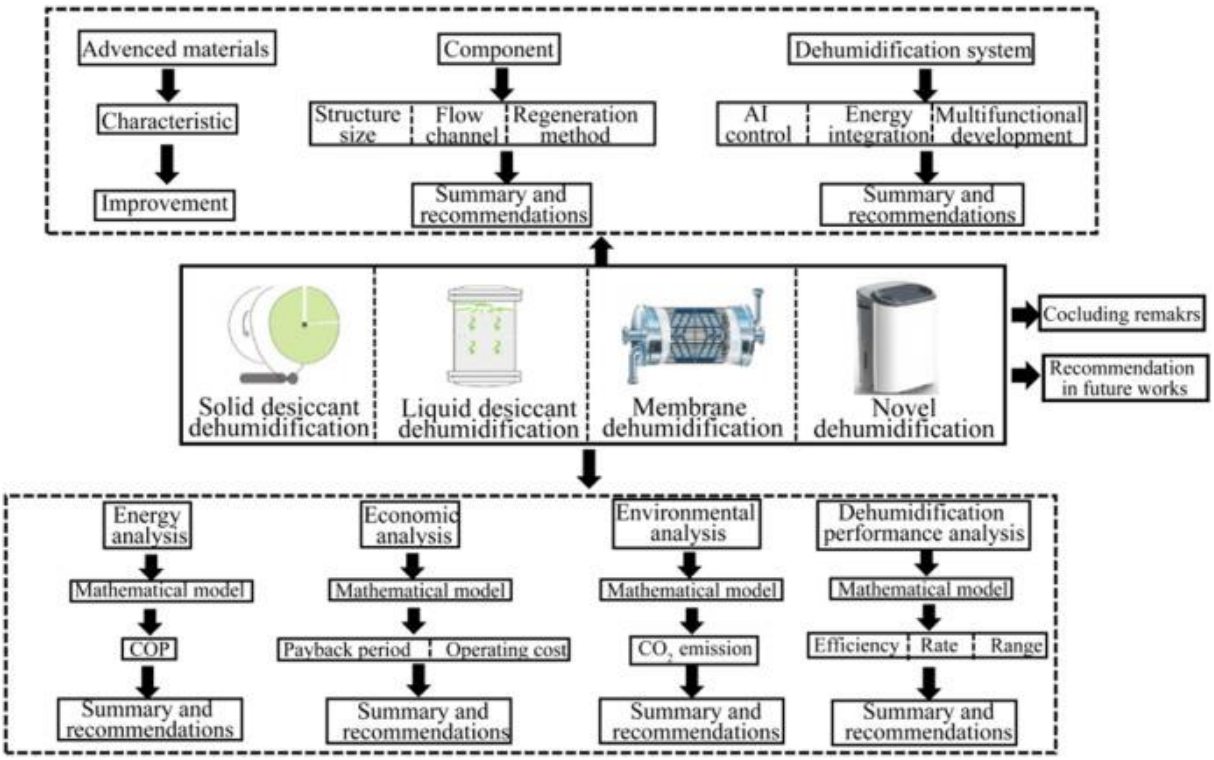


Fig. 2. Schematic representation of review methodology in deep dehumidification research.

## 2. Evaluation models of dehumidification system

The research methodologies for dehumidification-hybrid air conditioning systems mainly consist of experimental approaches and simulation techniques. The dehumidification, regeneration, and cooling processes all utilize principles of energy and mass conservation to develop models for heat and mass transfer.

### 2.1. Dehumidification performance models

To enable the comparative analysis of dehumidification performance across various systems, three metrics are introduced for assessment: outlet humidity ratio, dehumidification rate, and dehumidification efficiency, which can be calculated using Eqs. (1), (2):

$$R_d = M_p(d_{p,in} - d_{p,out}) \tag{1}$$

$$\eta_d = \frac{d_{p,in} - d_{p,out}}{d_{p,in} - d_{equ,in}} \tag{2}$$

Where, $R_d$ is the dehumidification rate (moisture removal capacity), kg/s; $M_p$ is the flow rate of process air, kg/s; $d_{p,in}$ and $d_{p,out}$ are the humidity ratio of the process air at the inlet and outlet, respectively, g/kg; $d_{equ,in}$ is the air absolute humidity ratio in equilibrium with the inlet solution at its temperature and concentration, g/kg; $\eta_d$ is the dehumidification efficiency (effectiveness).

### 2.2.1. Energy models

The energy consumption of a dehumidification system primarily originates from components such as compressors, fans, and regeneration heaters. To account for the energy consumption and COP (coefficient of performance) of the dehumidification system, the energy models are provided below:

$$COP_t = \frac{Q_t}{W_t} \tag{3}$$

$$Q_i = M_i C_p \Delta t_i \tag{4}$$

$$COP_{latent} = \frac{M_p C_p (d_{p,in} - d_{p,out})}{W_{latent}} \tag{5}$$

Where, $COP_t$ is the coefficient of performance of the total dehumidification system; $Q_t$ is the total energy consumption of the heat exchange, kW; $W_t$ is the energy consumption by heating, cooling, and dehumidification, kW; i is the gas to be tested, consisting of process air

and regeneration air; $C_p$ is the specific heat capacity, kJ/(kg·K); $W_{latent}$ is the energy consumption of latent heat, kW; $COP_{latent}$ is the coefficient of latent heat performance for the dehumidification system.

### 2.1.2. Economic models

The economic viability of a dehumidification system is primarily assessed by comparing the amount of moisture removed per unit of electrical power consumption and the payback period for different systems, as presented below:

$$R_e = \frac{C_e}{R_d} \tag{6}$$

$$P_p = \frac{I}{S - C_e \cdot p_e - \sum C_x \cdot p_x} \tag{7}$$

Where, $R_e$ is the water removal value - per unit electricity, kJ/g; $C_e$ is the electricity power consumption, kWh; $P_P$ is the payback period, year; I is the initial investment, $; $p_e$ is the electricity price, $/kWh; x is conventional energy, which includes coal, natural gas, and etc; $C_x$ is the conventional energy consumption; $p_x$ is the conventional energy price.

### 2.1.3. Environmental models

The environmental performance of a dehumidification system is primarily assessed by comparing the levels of $CO_2$ emissions from different systems, as presented below:

$$m_{CO_2} = C_e \cdot EF_e + \sum C_x \cdot EF_x \tag{8}$$

Where, $m_{CO_2}$ is the $CO_2$ emissions, kg; $EF_e$ is the carbon emission factor of electricity, kg$CO_2$/kWh; $EF_x$ is the carbon emission factor of conventional energy.

## 3. Deep dehumidification technology

### 3.1 Air compression dehumidification

The principle underlying air compression dehumidification is that, during the compression process in the air compressor, moist air condenses into liquid water. When subjected to wet air

pressure, the value of $d_{pout}$ decreases accordingly. The pattern of alteration in air humidity ratio persists even as the air pressure rises from 0.2 MPa to 0.6 MPa, as depicted in Fig. 3. The inlet air humidity ratio decreases from 3.2 g/kg to 1.2 g/kg in the LiBr solution dehumidification system and from 3 g/kg to 1.1 g/kg in the LiCl solution dehumidification system. In high-temperature and high-humidity environments, it is essential to cool and pre-dehumidify the compressor inlet in order to ensure the safe and energy-efficient operation of air compressors. In order to achieve more profound dehumidification, researchers have utilized techniques including refrigeration dehumidification and the combination of dehumidifiers with air compression technology.

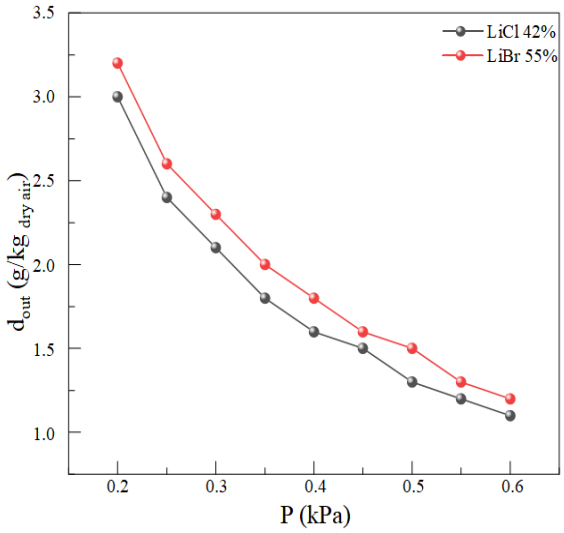


*Fig. 3. Effect of air pressure on outlet air humidity ratio.*

### *3.1.1. Compressed air hybrid refrigeration dehumidification*

When the temperature of compressed air rises, it is often necessary to employ compressed dehumidification in conjunction with refrigeration dehumidification. The schematic diagram of the compressed air refrigeration dehumidification system is depicted in Fig. 4. The ADL-5000W refrigerated compressed air dehumidifier, manufactured by China's KL Company, is capable of handling 510 $Nm^3$/min of air and consumes 90 kW of power [29]. At a pressure of 0.7 MPa, the pressure dew point may vary between 2 °C and 10 °C, while the atmospheric dew point may range from −25 °C to −17 °C. The process of compressing air results in a significant amount of heat generation, leading to an average outlet temperature of 110 °C. Yang et al. [30] introduced a cascade LiBr/$H_2O$ absorption refrigeration/transcritical $CO_2$ system designed to utilize 90–150 °C low-grade waste heat. When the temperature of the driving source decreases, there is a sharp decrease in COP. Moreover, exceeding a LiBr solution concentration of 60 % poses a risk of crystallization [31]. The payback period for the LiBr–$H_2O$ double evaporation-absorption heat pump is less than 2 years, and the maximum COP could reach 1.95. In order to

improve operational efficiency, it is important to evaluate the impact of $H_2O$–LiBr absorption chillers on waste heat recovery, the need for a heat source in an adsorption refrigeration system, the economic payback period, energy, exergy, and thermoeconomic analysis, as well as the cooling and heating performance.

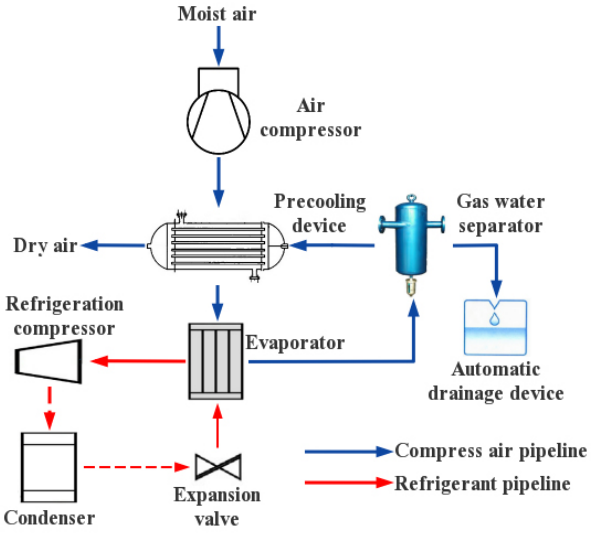


Fig. 4. Conceptual diagram of compressed air hybrid refrigeration dehumidification system.

### *3.1.2. Compressed air hybrid solid desiccant dehumidification*

Solid desiccants, due to their high adsorption capacity, have the potential to reach dew point temperatures as low as −50 °C or even lower [32]. To attain lower dew point temperatures, the use of solid desiccant dehumidification technology with compressed air is frequently utilized [33]. High-flow compressed air technology is frequently utilized in industries such as chemical production. In such applications, the presence of dust particles in the air compressor and inlet can lead to the condensation of moisture, causing the particles to become wet. This may lead to the hindrance of the efficient functioning of the desiccant wheel [34]. The presence of dissolved acidic pollutants can lead to the corrosion of the internal components of the impeller. Compressed air hybrid solid desiccant dehumidification systems are frequently utilized in a packed bed configuration, as illustrated in Fig. 5. Chen et al. [35] employed a UIO-66 (MOF) desiccant to dehumidify the moist compressed air, resulting in a dew point temperature ranging from −20 °C to −30 °C. Subsequently, a zeolite desiccant was employed to further reduce the dew point to −40 °C to −70 °C under conditions of low relative humidity. The strong interaction between zeolite and $H_2O$, along with its capacity to absorb water without causing damage to the crystal structure, enables it to maintain a high adsorption capacity even at low humidity and high temperatures. Zhang et al. [36] proposed a compressed air hybrid solid desiccant dehumidification system, which consisted of two adsorption devices filled with activated alumina particles. The system attained an outlet humidity ratio of less than 0.39 ppm (0.38 g/m$^3$) at a dew point temperature of −70 °C. Notably, the payback period for the investment in this system was exceptionally short, at 0.55 years. However, a difficulty emerged when employing adsorbent materials with elevated regeneration temperatures, as there could

be a discrepancy between the regeneration heat available and the necessary driving heat. This discrepancy has the potential to impact the efficiency of dehumidification. External factors such as meteorological conditions and load demand exerted a notable impact on the efficiency of the compressed air system. Under the specified working conditions of 0.60 MPa pressure and 39.7 % relative humidity of the inlet air, it was observed that for every 10 °C rise in inlet air temperature, the energy demand of the air compressor increased by 5.3 % and the energy efficiency decreased by approximately 5.3 % [37]. A compressed air energy storage system serves as an efficient approach for mitigating load fluctuations and facilitating peak shaving. Huang et al. [38] introduced a variable-speed compressed air energy storage system based on a double-fed induction machine, which has the potential to improve off-design energy efficiency by 6 %. Guo et al. [39] investigated the transient characteristics and control methodology of a compressed air energy storage system with the objective of reducing load balancing time and minimizing load overshoot.

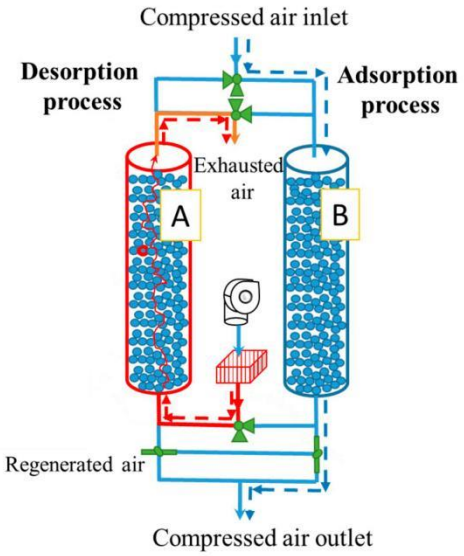


Fig. 5. Conceptual diagram of compressed air hybrid solid adsorption bed system [35].

### *3.1.3. Compressed air hybrid liquid desiccant dehumidification*

The dew point of the supply air in a liquid desiccant dehumidification system usually falls within the range of −20 °C–0 °C [40]. To attain reduced humidity levels and increased mass transfer, it is essential to utilize the suitable flow rates of compressed air and liquid desiccant. The diagram illustrating the configuration of the compressed air hybrid liquid desiccant dehumidification system can be observed in Fig. 6. The dehumidification performance of the system will rapidly increase when air is compressed, as demonstrated in Eq. (9). Elevated pressure amplifies the interface disturbance between the solution and the air, thereby augmenting the driving force for mass transfer. It is essential to dynamically assess the pressure fluctuations' intensity in compressed air liquid desiccant systems, vapor locks at the interface,

and the restoration of pressure in the trapped pores. Additionally, it is important to consider the effect of water/air ratio and the sensitivity of air/moist non-equilibrium phase transition cooling to transient characteristics.

$$d_{surface} = 0.622 \frac{P_v}{P - P_v} \tag{9}$$

where $d_{surface}$ is air humidity ratio of the saturated air layer on the surface of the solution, g/kg; $P_v$ is water vapor partial pressure of the saturated air layer on the surface of the solution, kPa; and P is system operation pressure, kPa.

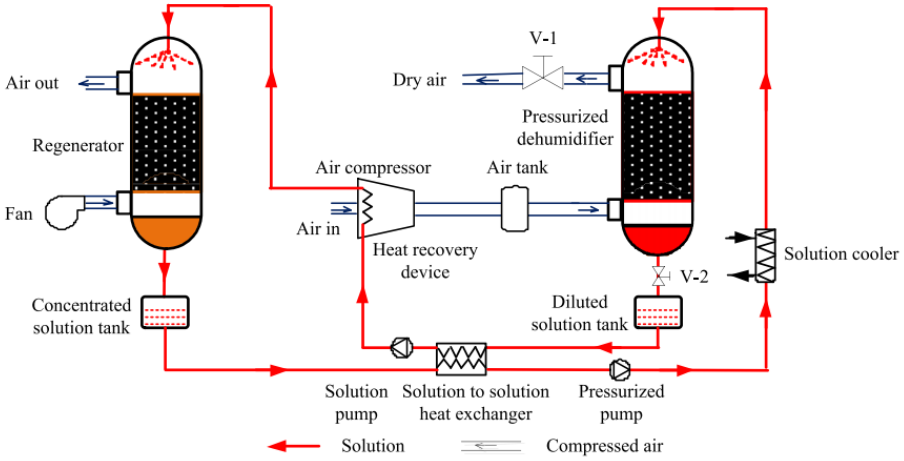


Fig. 6. Schematic chart of compressed air hybrid liquid desiccant dehumidification system [41].

The size of the equipment and the efficiency of dehumidification are significantly influenced by the ratio of liquid desiccant-to-air flow rate. A significantly large installation space would be necessary for the regeneration unit if the liquid desiccant-to-air flow rate ratio is set at a high value. In terms of investment and maintenance expenses, this may not be deemed acceptable. The performance of the compressed air hybrid liquid desiccant dehumidification system, including its COP and dehumidification capacity, deteriorates rapidly as the ratio of liquid desiccant to air decreases. A lower liquid desiccant-to-air ratio accelerates the regeneration rate, whereas a higher ratio promotes dehumidification [42]. Fang et al. [43] introduced a multi-stage internally cooled liquid desiccant dehumidifier with a liquid desiccant-to-air flow rate ratio ranging from 0.05 to 0.18, which is lower than the typical range of 0.25–2.5. The maximum experimental latent effectiveness reached 1.02, representing a two-fold increase compared to that of existing dehumidifiers. Naik and Muthukmar [44] introduced a mixed logistic regression model to forecast the variation in specific humidity within the dehumidifier and regenerator systems, based on operational parameters such as inlet desiccant concentrations and temperature, inlet air temperature, humidity ratio, and liquid desiccant-to-air flow ratio. The careful selection of the airflow configuration has a significant impact on the efficiency of

heat and mass exchange. Flow types encompass parallel flow, counter-flow, and cross-flow. Significantly, the efficiency of the counter-flow module exceeded that of the cross-flow type by almost 10 % [13]. The cross-flow configuration led to increased mixing and turbulence, which in turn improved dehumidification performance by 4–8% compared to the parallel flow configuration [162]. Accurate correlations for mass transfer between liquid desiccant and air are crucial for the operation of the system. Qi et al. [45] introduced a new mass transfer correlation with improved predictive accuracy (20%–30 % overall prediction errors), taking into account flow dynamics, the Marangoni effect, and the conditions of liquid/air contact that influence interface characteristics and wetting factors. This approach aims to address the limitations of existing mass transfer correlations based on experimental data. The contact area between the liquid and air, as well as the instability of the film, were observed to increase with higher liquid Reynolds numbers. By reducing the contact angle from 90° to 10°, the wetting factor almost doubles, resulting in a significant enhancement in mass transfer efficiency. This occurs despite the modest increase in the Sherwood number due to the suppression of film instability.

Table 4 provides a comprehensive summary of compressed air liquid desiccant dehumidification systems. Utilizing waste heat from an air compressor can facilitate the regeneration of the liquid desiccant at a temperature of 70 °C [46]. The heat required for regeneration constituted approximately 30 %–35 % of the waste heat that was available [41]. The values for $W_c$ and $R_E$ in this system were 10.1 % lower and 0.52 kJ/g lower, respectively, compared to those of the compressed air hybrid refrigeration dehumidification system operating at a pressure of 0.3 MPa [47].

Table 4. Summary of research on the compressed air hybrid liquid desiccant dehumidification system.

| Solution type | Humidity ratio | Atmospheric dew point | Pressure dew point | Application | Energy consumption | Reference |
|---|---|---|---|---|---|---|
| LiCl (0.8 MPa, 46 %) | 2.2 g/kg | −29.1 °C | −7.7 °C | Industrial gas | $W_{latent}$: 0.46 kW | [41] |
| LiBr (0.8 MPa, 58–63 %) | 1.05 g/kg | −28.34 °C | −6 °C | Low dew point industrial scenarios | $COP_t$: 2.254 | [48] |
| LiCl (0.5 MPa, 34–40 %) | 0.9 g/kg | −19 °C | −1 °C | Pneumatic and measuring instruments | Ce: 1.35 kW Re: 9.74 kJ/g | [47] |

### 3.2 Liquid desiccant dehumidification

### *3.2.1. Liquid desiccant materials*

Liquid desiccant systems mitigate irreversible losses and demonstrate favorable thermodynamic effectiveness across a broad spectrum of air treatment conditions. The principle of liquid desiccant dehumidification is grounded in the disparity between the saturation vapor pressure of water vapor at the surface of the desiccant solution and the saturation vapor pressure of water vapor in the air at the equivalent temperature. The oxygen-containing functional group of water in the adsorption layer is oriented in the "oxygen-down" configuration, and as additional water molecules are adsorbed, clusters of hydrogen bonds are formed [49]. The disparity in vapor pressure facilitates the movement of water molecules from the atmosphere to the desiccant solution, leading to the dehumidification of the air. The surface vapor pressure of a solution is influenced by both its temperature and concentration, as illustrated in Fig. 7. An increase in the temperature of the solution or a decrease in its concentration results in a corresponding increase in the surface vapor pressure. Wang et al. [50] conducted a study on the small-scale liquid desiccant dehumidification process, highlighting the importance of considering the interconnected processes of absorbent heating and volume expansion in liquid dropout. The study reveals that the droplet growth rate and final expansion ratio are influenced by the relative humidity and ambient temperature.

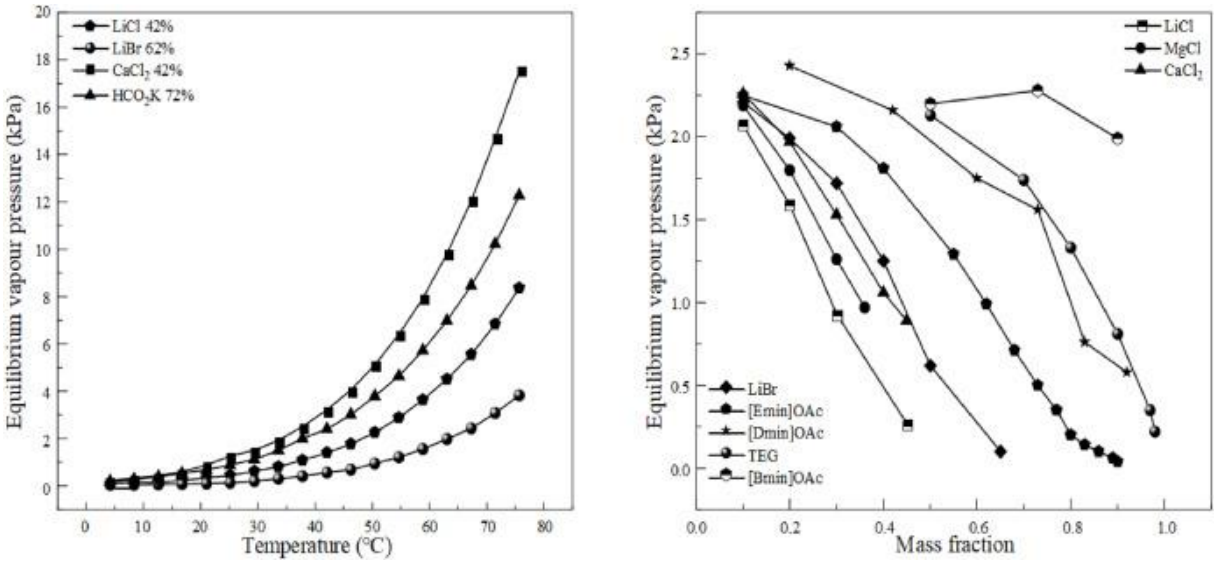


Fig. 7. Relationship between temperature, mass fraction, and equilibrium vapor pressure in dehumidification [51].

Table 5 presents a comprehensive overview of the parameters related to liquid desiccants. During the initial years, dehumidification systems utilized a solution of triethylene glycol (TEG). However, the system's stability was compromised as a result of the elevated viscosity of TEG [53]. Consequently, it is being gradually substituted by metal halide solutions such as LiCl, LiBr, and $CaCl_2$. At identical temperatures, the dehumidification efficiency can be ordered from highest to lowest as follows: LiCl > LiBr > $CaCl_2$ [54,55]. The addition of phase-change materials to an aqueous LiCl desiccant is a significant approach for enhancing dehumidification efficiency. The vapor pressure of the mixture is determined to be 36.4 % lower than that of the

pure LiCl desiccant [56]. $CaCl_2$ demonstrates a relatively high equilibrium vapor pressure when exposed to high-temperature conditions. However, its extensive use is constrained by the unstable conditions that are contingent upon the inlet conditions of air and solution [57]. Owing to the propensity of metal salts to undergo crystallization, corrosion, and related issues, the use of weak acid salts like KCOOH, $CH_3COOK$, and $CH_3COONa$ has been adopted for liquid dehumidification. At temperatures ranging from 45 °C to 65 °C, the vapor pressure of a KCOOH solution with a concentration of 64.3 wt% to 74.3 wt% is comparable to that of a LiCl solution with a concentration of 33 wt% to 38 wt% [58]. However, weak acids are limited in their capacity to dehumidify due to their high vapor pressure values, even when compared to solutions of LiCl and LiBr at equivalent concentrations. In a single solution, there are unavoidable disadvantages, including corrosion, high vapor pressure, instability, and expense. The composition of the composite solution offers a novel approach for enhancing the dehumidification efficiency of liquid desiccants. For instance, the dehumidification efficiency of LiCl/$CaCl_2$ solution blend exceeds that of LiCl solution by over 20 % [59].The optimal concentration ratio for the mixed solution was determined through experimental investigation [57]. Zhao et al. [60] conducted a comparison of the dehumidification performance of various composite liquid desiccants and found that LiCl–$MgCl_2$ solution exhibited the highest dehumidification performance at equivalent concentrations. Li [61] carried out experimental research utilizing TEG-LiCl solution, PG-LiCl solution, TEG-LiBr solution, and PG-LiBr solution. The vapor pressure of the composite solutions was determined to be lower than that of the individual organic solutions, providing additional evidence for the potential use of organic-salt mixed solutions as desiccants in liquid dehumidification systems.

Table 5. Comparative analysis of parameters across different liquid desiccants [40,46,52].

| **Solution type** | **Dew point temperature (°C)** | **Concentration (%)** | **Toxicity** | **Corrosiveness** | **Stability** | **Price ($/ton)** | **Appliance** |
|---|---|---|---|---|---|---|---|
| $CaCl_2$ | -3 to −1 | 40–50 | No | Medium | Stable | 284–721 | Urban gas |
| DEG | −15 to −10 | 70–95 | No | Weak | Stable | Higher than saline solution | General gas |

| Solution type | Dew point temperature (°C) | Concentration (%) | Toxicity | Corrosiveness | Stability | Price ($/ton) | Appliance |
|---|---|---|---|---|---|---|---|
| Gycerol | 3 to −15 | 70–100 | No | Weak | Oxidative decompositio | – | Industry gas |
| Phosphoric acid | −15 to −4 | 80–95 | Yes | Strong | Stable | – | Laboratory hygroscopic ag |
| Caustic soda Caustic calcium | −10 to −4 | – | Yes | Strong | Stable | – | Industrial compressed gas |
| Sulfuric acid | −15 to −4 | 60–70 | Yes | Strong | Stable | – | Chemical devic |
| LiCl | −20 to −5 | 30–50 | Yes | Medium | Stable | 7400–8418 | Textile, pharmaceutical |
| LiBr | −20–0 | 25–65 | Yes | Strong | Stable | 3316–3660 | Pharmaceutical laboratory |

Ionic liquids have garnered attention in research due to their exceptionally low vapor pressure, non-crystallizability, and low corrosiveness. Under comparable circumstances, [EMIM]BF4 and [Dmim]OAc demonstrate marginally reduced dehumidification efficacy in comparison to LiBr solutions [62,63]. However, the enhancement of dehumidification performance could be achieved by increasing the mass concentration of the ionic liquid solution. Li et al. [64] enhanced the dehumidification efficiency of LiBr and LiCl solutions through the addition of an ionic liquid. The results indicated that the inclusion of [Dmim]Cl had a more pronounced impact in comparison to [Dmim]BF4. Nevertheless, the practical utilization of ionic liquids is constrained by their elevated viscosity, degradability, and toxicity [65].

The induction of the Marangoni effect through the addition of specific chemical surfactants or coating hydrophilic materials to the liquid desiccant can reduce the contact angle and increase the wetting area, thus enhancing the efficiency of water vapor absorption [66]. However, the majority of current surfactants possess odors, are toxic, and are not suitable for direct use in air dehumidification applications. Wen et al. [67,68] conducted a study on a novel non-volatile, odorless, and non-toxic surfactant (PVP–K30), which demonstrated the ability to enhance both $R_d$ and $\eta_d$ by 22.7 % and 19.9 %, respectively, with the addition of only 0.4 % of PVP-K30. Dong et al. [69] performed experimental research to investigate the impact of $TiO_2$ coating on the reduction of the contact angle of the solution from 84.6° to 8.8°, as well as the increase in the values of $R_d$ and $\eta_d$ by 1.60 and 1.63, respectively. Simultaneously, it has the potential to achieve an annual 5.7 % reduction in electricity expenses compared to structures lacking $TiO_2$ coating. The uniform dispersion of nanofluids in liquid dehumidifiers has been shown to significantly enhance heat and mass transfer capabilities [70]. Wen et al. [71,72] utilized

mechanical and chemical techniques to disperse multiwall carbon nanotubes in LiCl solutions, resulting in an average relative enhancement of 25.9 % for nanofluids in dehumidification and 24.7 % in regeneration. Low-temperature liquid desiccants exhibit a reduced surface vapor pressure. Low-temperature conditions enhance the driving force and prolong the duration of interaction between the solution and air [73]. Similar to ambient atmospheric temperatures and high-concentration solutions, low temperatures and low-concentration liquid desiccant solutions have the capability to dehumidify [74]. Zhang et al. [75,76] conducted a study and noted that as the specific heat ratio between air and solution approaches 1, it improves both heat and mass transfer capabilities. The adjustment of solution flow rates in both the dehumidifier and regenerator units could be accomplished by utilizing two pumps with different rated flow capacities to tackle heat and mass transfer concerns [23]. A higher flow rate of the solution contributes to improved dehumidification performance; however, it is important to carefully consider the balance between $\eta_d$ and pump power consumption.

### *3.2.2. Components and systems*

Fig. 8 depicts the flowchart of the liquid desiccant dehumidification system. Various types of liquid regenerators encompass packed beds, falling film, spray water, and membrane-based configurations. In order to enhance the dehumidification effectiveness of liquid desiccants, researchers have utilized a variety of approaches to achieve more thorough dehumidification.

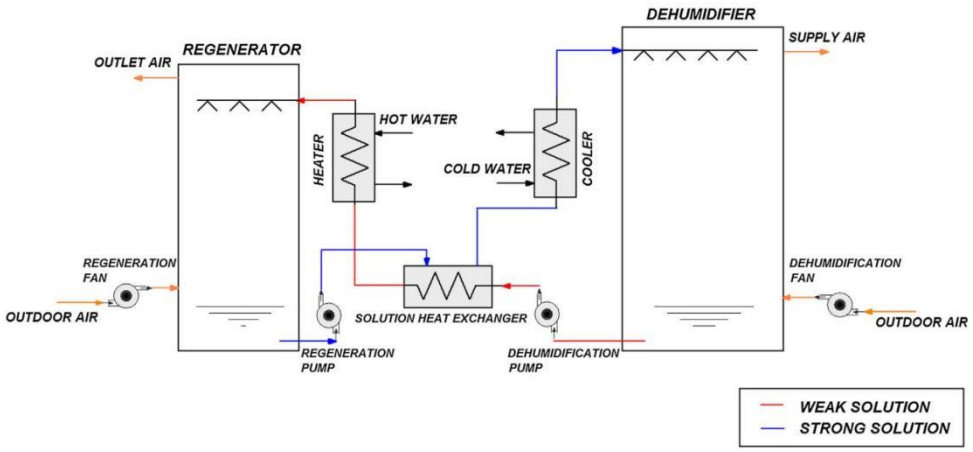


Fig. 8. Conceptual diagram of liquid desiccant dehumidification system [77].

Internal cooling dehumidifiers have the potential to significantly lower the regeneration temperature of solutions, as well as reduce air pressure drop and droplet transport [78,79]. Shah et al. [80] performed an experimental investigation to compare the dehumidification effectiveness of adiabatic dehumidifiers and internally cooled dehumidifiers using a $CaCl_2$ liquid dehumidifier concentration of 40 %, with $\eta_d$ value of 67 % and 95 %, respectively. Lun et al. [81] introduced a self-cooling method by incorporating absolute ethanol into LiCl solution to uphold a consistent temperature.

The droplets are dispersed into the regeneration chamber via the intense vibration and atomization of the ultrasonic transducer, thereby substantially increasing the surface area

for heat and mass transfer. Yang et al. [82] employed ultrasonic atomization technology, which resulted in a 4.4 °C reduction in regeneration temperature and a 23.4 % decrease in energy consumption during the regeneration process. Yang et al. [83] proposed the integration of an internal cooling system with an ultrasonic atomization liquid desiccant system and defined a suitable cooling power range to enhance cost-effectiveness. Nevertheless, the limitations resulting from ultrasonic atomization, which transports droplets, have hindered its widespread implementation and require further validation.

Multi-stage solution dehumidifiers exhibit higher exergy efficiency and a lower outlet humidity ratio compared to single-stage solution dehumidifiers [84]. Peng and Zhuo [85] introduced a hybrid-connected double-stage dehumidifier system. The system employed a $CaCl_2$ solution for pre-dehumidification, whereas LiCl solution was used for deep dehumidification experiments. The regeneration temperature experienced a decrease of 12.2 °C, leading to a slight improvement in the exergy efficiency of the system [86,87].

## 3.3. Solid desiccant dehumidification

### *3.3.1. Solid desiccant materials*

Solid desiccants eliminate moisture by adsorbing it into their surface pores, with two primary categories identified: physical adsorption and chemical adsorption. During physical adsorption, the adsorbate molecules predominantly establish hydrogen bonds with the surface of the adsorbent, resulting in the interaction of van der Waals forces between the molecules during the physical adsorption [88]. In contrast, solid desiccants like calcium chloride and lithium chloride remove moisture by transforming into crystalline hydrates and forming adsorption chemical bonds.

Table 6 provides a comprehensive summary of solid desiccant parameters. Silica gel has been extensively utilized due to its cost-effectiveness, although it is recognized for its comparatively lower adsorption capacity and higher adsorption heat [89]. Activated carbon demonstrates a specific water vapor adsorption capacity only at elevated relative humidity levels, and it is rarely utilized as a sole material for dehumidification [90]. Activated alumina, due to its high affinity for water, has the capability to reach a low dew point temperature of below −70 °C and is frequently employed as an industrial catalyst [91]. Zeolites and molecular sieves demonstrate strong adsorption capabilities in high-temperature and low-humidity environments, allowing for the purification of air to achieve exceptionally low humidity levels and dew point temperatures ranging from approximately −40 °C to −60 °C [92]. The desorption process presents a comparatively greater challenge, as the regeneration temperature is higher than that required for silica gel and activated alumina [93]. In contrast to physical desiccants, chemical desiccants such as metal salts exhibit strong moisture absorption capabilities. However, upon adsorption, they experience deliquescence, leading to the formation of solutions that have the potential to cause corrosive effects on metals [94]. In order to mitigate corrosion and instability caused by material deliquescence, it is feasible to enhance the adsorption capacity by 10 %–40 % through the dispersion of silica gel in a small amount of metal salt materials [95,96]. Nevertheless, an excessive quantity of metal salt materials could potentially overwhelm the sealing system during the sorption process, resulting in corrosion and leakage, thereby significantly constraining the sorption capacity.

Table 6. Comparative analysis of parameters across different solid desiccants [71,72,89,97,98].

| Solid desiccant | | Test conditions | Adsorption capacity (g/g) | Regeneration temperature (°C) | Specific surface area ($m^2/g$) |
|---|---|---|---|---|---|
| **Silica gel** | | **30 °C, 60 % RH** | **0.1–0.3** | **70–150** | **300–800** |
| Molecular sieve/Zeolite | NaX | 30–40 °C, 60 % RH | 0.34 | 250–350 | 400–750 |
| | NaY | 25 °C, 80 % RH | 0.25 | | |
| | NaA | 25 °C, 60 % RH | 0.23 | | |
| | YZSM-20 | 25 °C, 80 % RH | 0.28 | | |
| Activated carbon | ACY-60 | 27 °C, 60 % RH | 0.18–0.29 | 70 | 500–1500 |
| | ACs | 25 °C, 60 % RH | 0.25–0.50 | – | |
| Composite | Silica gel-Activated carbon-$CaCl_2$ | 27 °C, 9 % RH | 0.23 | – | 1117 |
| | $Al_2O_3$–$SiO_2$ | 23 °C, 50 % RH | 0.19 | – | – |
| | $CaCl_2$/Silica gel | 35 °C, 4 % RH | 0.19 | 60–80 | – |
| | $CaCl_2$-MCM-41 | 25 °C, 70 % RH | 0.75 | 90–130 | 325 |
| | MIL-101(Cr)-graphite oxide | 25 °C, 90 % RH | 1.58 | 60 | – |
| MOFs | MIL-101(Cr) | 30 °C, 60 % RH | 1.5–1.7 | 70–80 | 3000–4000 |
| | MIL-101(Fe) | 30 °C, 60 % RH | 0.84 | 70–80 | 1549 |
| | MIL-100(Al) | 30 °C, 60 % RH | 0.75 | 70–80 | 1814 |

| Solid desiccant | | Test conditions | Adsorption capacity (g/g) | Regeneration temperature (°C) | Specific surface area ($m^2/g$) |
|---|---|---|---|---|---|
| **Silica gel** | | **30 °C, 60 % RH** | **0.1–0.3** | **70–150** | **300–800** |
| Others | Dried coconut shell | 32 °C, 75 % RH | 0.30 | – | – |
| | Dried durian peel | 32 °C, 75 % RH | 0.17 | – | – |

The novel MOF-74 (Ni) with expanded benzene rings was developed by Pacific Northwest National Laboratory [99]. MOF material demonstrated not only a water adsorption capacity of 0.9 g/g and an adsorption capacity of 0.8 g/g for the refrigerant R134a. Zeng et al. [100] introduced a thermally responsive material that demonstrated temperature-dependent adsorption isotherms for water vapor, departing from the conventional fixed affinity. The material exhibited improved dehumidification performance in comparison to silica gel desiccants, resulting in a 30 % decrease in energy consumption for dehumidification. Materials scientists have developed water-absorbing polymers using acrylates and acrylamide, which have demonstrated a water absorption capacity of 2–3 times their initial weight [101,102]. The addition of metal salts resulted in a 2–3 times increase in the adsorption capacity of these polymers compared to the raw materials [103]. Dai et al. [104] developed a nanostructured moisture-absorbing gel dehumidification material that demonstrated an adsorption capacity of up to 1.58 g/g. The dehumidification time required to achieve the same level of dehumidification was shorter when compared to the 4A molecular sieve and silica gel. Vivekh et al. [105] developed a composite polymer desiccant that consists of polymers containing hydrophilic and hygroscopic salts. This desiccant demonstrated a 12-fold higher isothermal water absorption capacity compared to silica gel, zeolite, and MOFs. Additionally, it was capable of undergoing condensation heat regeneration at temperatures ranging from 40 °C to 50 °C. However, the synthesis of such materials presents challenges and high costs, resulting in many of them remaining in the experimental phase. Additionally, there exist environmentally sustainable desiccants, including agricultural waste and other biomass materials, which, following appropriate processing, demonstrate specific dehumidification properties [106]. The desiccants were generally unsuitable for deep dehumidification due to their relatively weak adsorption capacity, despite their cost-effectiveness, biodegradability, and environmental friendliness.

The adsorption capacity is influenced by the thickness of the desiccant layer. If the desiccant layer is too thin, the contact time may be insufficient for adequate adsorption to take place. Conversely, a greater thickness of the adsorbent layer typically results in enhanced dehumidification performance. For instance, a rise in thickness from 0.05 mm to 0.2 mm has been shown to enhance dehumidification performance by 113 % [107]. However, the

augmented thickness led to a corresponding increase in resistance, leading to notable pressure drop losses and reduced energy efficiency [108]. The stress applied across the material is a result of thermal expansion and contraction, as well as the binding and releasing of water molecules into and out of the desiccant microstructure. These conditions contribute to the generation of stress within the material. Therefore, it requires long-term material and performance stability, as well as favorable water sorption uptake, isotherms, and kinetics. The diagram illustrating the solid desiccant dehumidification system can be found in Fig. 9. The energy required for regenerating solid dehumidification systems is relatively high. Efforts to minimize energy usage during the process of desiccant regeneration are currently a key area of research.

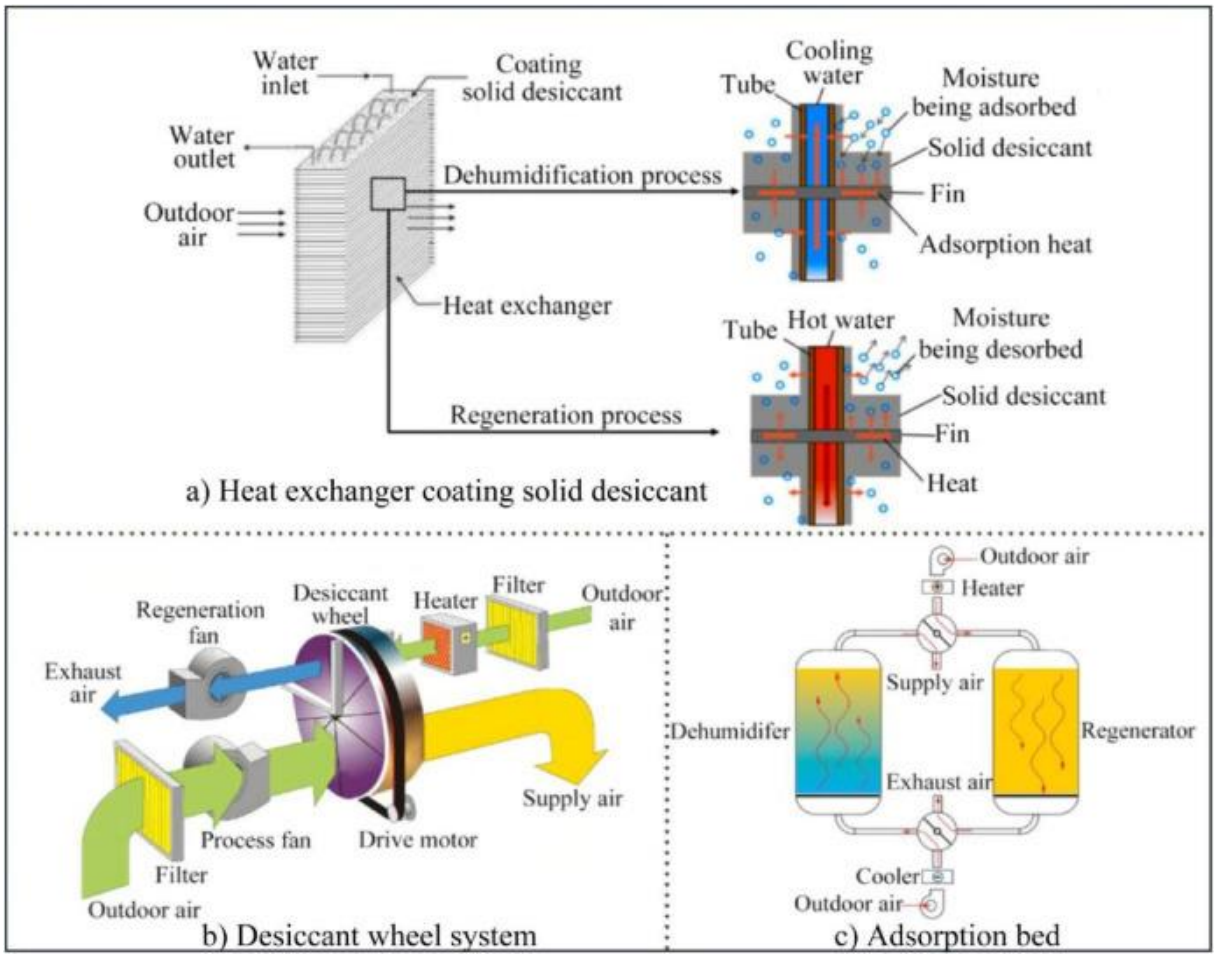


Fig. 9. Conceptual diagram of solid desiccant dehumidification system [32,109].

As indicated in Table 7, the techniques for regenerating solid desiccants primarily encompass waste heat regeneration [110], solar energy regeneration [111], and ultrasonic regeneration [112]. Unstable conditions in low-grade heat sources can potentially diminish the dehumidification performance within the dehumidification system [113,114]. Electrically-driven regeneration, a novel method of regeneration, has faced limitations in its performance development as a result of bubble effects and electrode erosion [115]. The use of microwave and ultrasound has been shown to effectively enhance the regeneration capacity of desiccants

and reduce the duration of the regeneration process [116]. Utilizing free renewable energy and waste heat resources can lead to a significant reduction in operational expenses.

Table 7. Summary of studies on the regeneration methods.

| Reference | Method | Regeneration description | Results |
|---|---|---|---|
| [113] | Experiment | Ultrasonic power and thermal power regeneration silica gel | 5 W Ultrasonic power and 20 W thermal power<br>Short regeneration time and strong regeneration ability<br>Regeneration temperature and energy reduced 2.7 °C and 26 %, respectively |
| [117] | Experiment | Microwave and solar radiation regeneration silica gel | Regeneration degree: 77.7 %<br>3.77 and 1.05 times higher than the solar regeneration and the microwave regeneration<br>Max energy efficiency: 19.4 % |
| [118] | Experiment | Electric furnace and microwave device regeneration activated carbons | Microwave regeneration was more rapid and efficient |
| [119] | Simulation | Purge gas regeneration | Optimum purge angle raised COP 30 %<br>Reduced regeneration energy: 22.7 %<br>Saving energy efficiency: 33 % |
| [120] | Experiment | Heat pump (engine exhaust gas) regeneration | Low regeneration temperature and precooling increased $\eta_d$<br>Exergy efficiency raised 31.5 % |
| [121] | Experiment | Thermal regeneration silica gel | When the regeneration heat decreased, the decreased in $\eta_d$<br>could be effectively suppressed by controlling the constant regeneration temperature mode of the desiccant wheel speed |
| [122] | Simulation | Solar radiation and waste heat regeneration | Solar radiation 1800 W/m$^2$<br>$\eta_d$<br>: 1–5 |

### *3.3.2. Desiccant coating heat exchanger*

The desiccant coating heat exchanger is primarily utilized for dehumidification in residential buildings due to constraints related to latent heat load and fresh air volume. The latent heat load consists primarily of three components: the human body, fresh air, and equipment. Desiccant-coated heat exchangers encompass fin-tube heat exchangers, wire-tube heat exchangers,

and microchannel heat exchangers. Fin-tube heat exchangers and microchannel heat exchangers are found to reduce heat transfer coefficients by 15 % and 30 % respectively, while also leading to an increase in pressure loss by 55%–60 % compared to conventional heat exchangers [123,124]. When the depth of the fin in the desiccant coating heat exchanger is increased from 44 mm to 88 mm, there is a 40 % increase in the moisture removal capacity and a 10 % increase in COP. A lower fin pitch results in increased resistance to airflow, necessitating a higher energy input to achieve the same flow rate. The mass transfer coefficient and moisture removal rate of microchannel heat exchangers exceed those of fin-tube heat exchangers by 15 % and 150 %, respectively. Fin and tube heat exchangers exhibit a maximum heat transfer coefficient that is lower than the minimum value of the heat transfer coefficient of metal foam [125]. In comparison to the heat exchanger coated with aluminum fumarate, the mass of adsorbate increased by 66.6 % in the heat exchanger coated with composite silica gel [126]. Zeolite-coated heat exchangers have been shown to achieve regeneration at 90 °C, with a moisture removal capacity 5.4 times that of conventional systems and a COP of 0.5 [127]. The utilization of sensible heat recovery in conjunction with desiccant coating heat exchange has been shown to enhance COP by an additional 13 % [128].

### *3.3.3. Adsorption bed*

The adsorption bed is primarily utilized in industrial dehumidification due to its simple design and ease of manufacturing. The increased irreversibility associated with multiple heat transfer resistances results in a reduced capacity of the adsorption bed compared to that of the desiccant-coated heat exchanger. The significant pressure drop requires the utilization of a high-capacity pump to facilitate flow and create additional space for the installation of equipment. The adsorption bed systems are classified into packed beds and fluidized beds based on the desiccant's movement and circulation status.

Optimizing the configuration of the adsorption bed is crucial for addressing the limitations associated with poor heat transfer capability and significant pressure drops. Ramzy et al. [129] introduced the concept of an intercooled packed bed and determined that by optimizing the axial position and the length ratio of the intercooling-adsorption bed to be between 0.45 and 0.65, the total adsorbed mass can be increased by 22 %. Shamim et al. [130] introduced a multilayer fixed-bed desiccant dehumidifier without binders, which resulted in a 98 % reduction in pressure drop and a 36 % increase in dehumidification efficiency. Yeboah and Darkwa [117] concluded that helically coiled oscillating heat pipes have the potential to improve heat and mass transfer. They also found that the annular bed exhibited a higher adsorption rate compared to the full bed. Liang et al. [131] introduced an enhanced circulating inclined fluidized bed system featuring a 20 cm particle channel and a 20° incline angle, which demonstrated superior dehumidification performance and occupied a smaller volume. The energy efficiency of this system exceeded that of the circulating erect fluidized bed systems by 77.9 % and the circulating inclined fluidized bed systems by 40.1 %.

### *3.3.4. Desiccant wheel*

Due to the continuous cycle, high desiccant material utilization, high efficiency, and low pressure drop, the adsorption bed is extensively employed for dehumidification in industrial

and building applications. Bhabhor and Jani [132] conducted a study on the dehumidification performance of various desiccant wheel channel types. They found that the sinusoidal geometry types resulted in a significant reduction in relative humidity of up to 80 %, with the average temperature of the supply air increasing by 38.98 %. This type of geometry was identified as the most effective in dehumidifying the supply process air. Multi-stage desiccant wheel dehumidification systems have been shown to effectively lower the regeneration temperature compared to single-stage desiccant wheel systems [133]. Tu and Hwang [134] carried out experimental research and discovered that decreasing the outdoor air humidity ratio from 19 g/kg to 4 g/kg resulted in regeneration temperatures of 101.7 °C and 72.7 °C for the single and double desiccant wheel systems, respectively. Asadi and Roshanzadeh [135] successfully reduced the required regeneration temperature of the desiccant wheel by 4.1 °C through the regulation of fresh air and return air volumes entering the first and second stages of the wheel. Moreover, there was a 15.5 % increase in COP and a 21.4 % increase in exergy efficiency. Tu and Hwang [134] conducted optimization by taking into account various area ratios, numbers of wheels, and proposed system configurations for diverse application scenarios, as presented in Table 8. The equation for $A_{ratio}$ is calculated as shown in Eq. (10):

$$A_{ratio} = \frac{A_p}{A_r} \tag{9}$$

Where, $A_{ratio}$ is the area ratio of desiccant wheel; $A_p$ is the area of process air, $m^2$ ; $A_r$ is the area of regeneration air, $m^2$.

Table 8. Optimal design configurations for desiccant wheel [134].

| $A_{ratio}$ | Number of desiccant wheel | System configuration |
|---|---|---|
| 1 | 3~4 | vapour compression cycle |
| 2 | 1 | Electric heater or natural gas burner |
| 1 | 1 ( NTU of heat recovery unit ≥ 2) | With heat recovery |
| 1 | 3~4 | Low regeneration temperature |
| 2 | 1 | Low $W_{latent}$ or high $COP_{latent}$ |

The process of solid desiccant dehumidification frequently entails an exothermic reaction. In order to minimize the production of adsorption heat and convert the adiabatic dehumidification process into an isothermal dehumidification process, researchers have utilized the internal cooling desiccant wheel configuration [81,136]. In comparison to conventional desiccant wheels, the dehumidification efficiency could be enhanced by 48 % [136,137]. However, this necessitated a sacrifice in air flow, as the maximum cross-sectional area for dehumidified air accounted for only 28 % of the total. This required a wheel with a diameter 89 % larger to handle the same air volume as the non-internal cooling configuration. In order to reduce the size of the double-stage desiccant wheel system, Ge et al. [138] suggested a dual-stage

dehumidification system with a single desiccant wheel. Dividing the desiccant wheel region into four sections reduced the system length, but it also resulted in increased complexity in the air ducts.

### 3.4. Membrane dehumidification

The membrane dehumidification method is a novel approach that exploits $H_2O$ selectivity difference between the two ends of the membrane as air flows over distinct membrane components. The water vapor permeability exceeds that of nitrogen, oxygen, and other gases by at least two times. By harnessing the selectivity of the membrane, it efficiently separates moist air from other gases, thereby achieving the separation of water vapor from dry air without generating heat. Following this, the dehumidified air can be cooled and subsequently circulated into the indoor environment with the use of a cooling apparatus.

The categorization of different membrane materials is depicted in Fig. 10. Membranes can be classified based on their physical structure and chemical properties, with pore sizes of 0.1 μm and dense membranes with pore sizes of 0.1 nm, respectively [15,139]. Membranes can be classified based on their membrane material into organic membranes (polymers), inorganic membranes (zeolites, ceramics, molecular sieves), and composite membranes. Membranes can be categorized into flat sheet membranes and hollow fiber membranes based on their membrane configuration. The flat sheet membranes have a thickness of approximately 100 μm, whereas the hollow fiber membranes have a diameter of around 500 μm [140]. Hollow fiber membranes offer several advantages, such as a larger surface area and more attractive aesthetics, enhanced heat transfer efficiency, and reduced pressure drop on the gas side. When compared to flat sheet membrane modules of half the size, hollow fiber membrane modules demonstrate equivalent dehumidification performance [141]. However, the construction of hollow fiber membranes presents greater challenges due to the requirements for sealing at both ends, and they are also more prone to particle fouling [142].

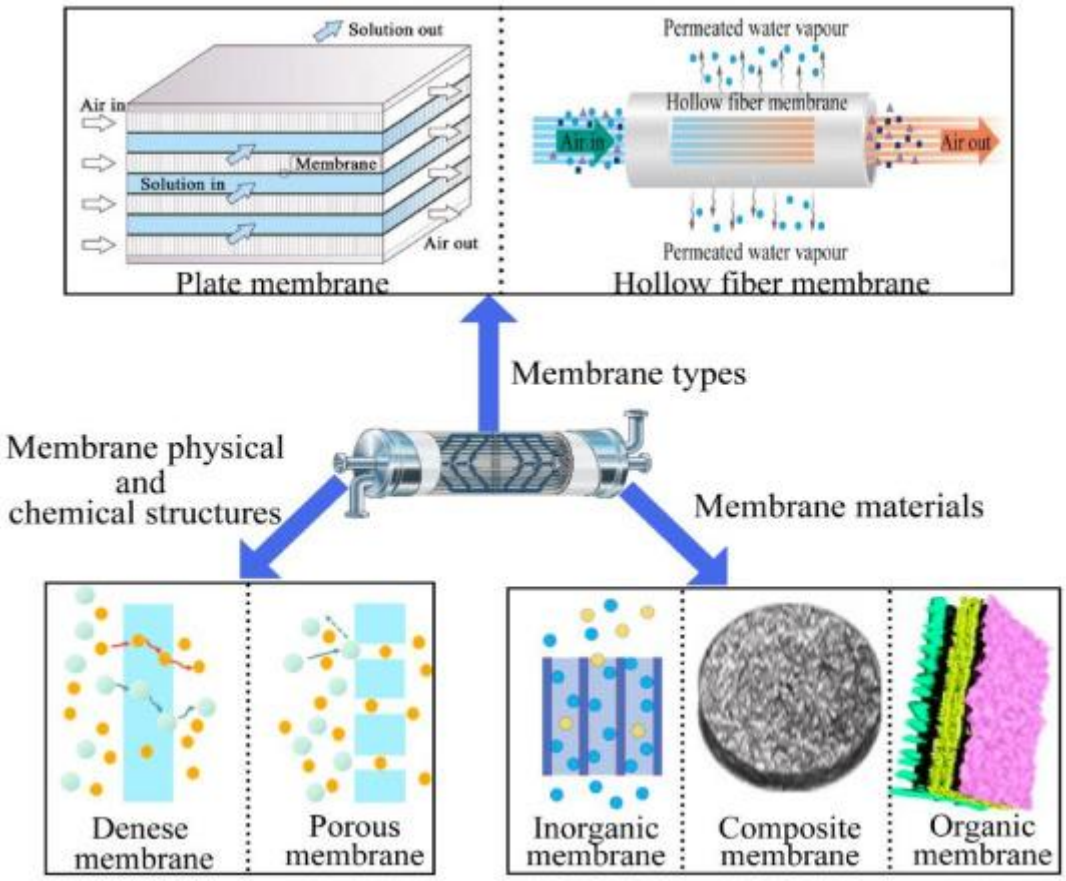


Fig. 10. Classification of different membranes.

As shown in Table 9, the permeability and selectivity of the membrane play a crucial role in determining the dehumidification performance. Membranes possessing greater selectivity could enhance the permeation of water vapor on the permeate side to a significant extent. The membrane exhibited a selectivity range of 178 to 16,300, with a preference for higher selectivity to mitigate solution leakage and carryover [15]. Membranes with high permeability exhibit reduced operating pressures, although they are susceptible to decreased selectivity [52]. Achieving the desired airflow and dehumidification level in the supply air with low energy consumption requires a delicate balance between permeability and selectivity. It is crucial to take into account the chemical reactions involved in certain designs, including heat and moisture transfers, water-vapor permeability complexes, high packing density, and selective permeability.

Table 9. Comparative analysis of different membrane material properties [15,141].

| Membrane description | Test conditions | Permeability mol/(m²·Pa·s) | $H_2O/N_2$ selectivity |
|---|---|---|---|
| PVA-LiCl with coating PEI hollow fiber membrane | 27–31 °C, 14.7–16.7 g/kg | $1.1 \times 10^{-6}$ | 4240 |
| PAN-PDMS hollow fiber membrane | 28–32 °C,18–22 g/m³ | $2.8 \times 10^{-6}$ –$4.3 \times 10^{-6}$ | 35–220 |
| PES-SPEEK composite hollow fiber membrane | 50–65 °C, RH: 44–90 % | $5.0 \times 10^{-7}$–$8.4 \times 10^{-7}$ | 190000 |
| PES hollow fiber membrane with coating polyamide | 30 °C, 30–32 g/m³ | $5.0 \times 10^{-7}$ | 500 |
| PES hollow fiber Membrane in Polyarmide Matrix of Carboxylated $TiO_2$ Nanoparticles | 30 °C,25–27 g/m³ | $4.5 \times 10^{-7}$ | 486 |
| PES hollow fiber membrane with coating CA/PEG | 30 °C, RH: 20 % | $1.5 \times 10^{-8}$ | 175.5 |
| Porous nickel sheet supported NaA zeolite flat membrane (zeolite/Ni) | 32 °C, RH: 90 % | $6.8 \times 10^{-6}$ | 178 |
| Ionic liquid [emim][$BF_4$] membrane | 31.4, 28.2 g/kg | $3.5 \times 10^{-7}$ | 16300 |
| Polysulfone hollow membrane | 32 °C, RH: 100 % | $1.8 \times 10^{-7}$ | 529 |
| Ionic liquid [emim][DCA] membrane | 25 °C, RH: 94 % | $1.3 \times 10^{-6}$ | 1000 |

The enhancement of water selectivity alongside the augmentation of permeability has been the subject of investigation by numerous polymer scientists. Various factors, including material composition, type, and structure (such as porosity, pore size, and thickness), have been found to exert influence on these properties. The improvement of water selectivity while increasing permeability has been studied by many polymer scientists, and various factors such as material, type, and structure (porosity, pore size, and thickness) influence these properties. As the membrane porosity and pore size increase and the membrane thickness decreases, the moisture content at the air outlet of the membrane module decreases, leading to an increase in dehumidification capacity and efficiency. However, this enhancement also brings about the potential for liquid permeation, thereby increasing the overall resistance to the mass transfer process [52]. Niu et al. [143] conducted a comprehensive analysis of the mechanical strength of membrane materials and determined that a membrane with a porosity of 0.8, a thickness of 0.1 mm, and a pore size of 180 nm exhibits the most effective dehumidification performance for crossflow parallel-plate membrane dehumidification. The inclusion of LiCl has the potential to enhance the mechanical properties of the membrane and also to augment its hygroscopic rate and capacity. The study shows that an increase in the concentration of LiCl leads to a significant improvement in the surface sealing of PVA/PEO polymer. Additionally, the shape of the polymer-formed film transitions from loose to firmly packed [144]. A greater concentration of polymer contributes to a more robust membrane structure, while a higher concentration of

cross-linker increases the density of spherical particles, both of which enhance the strength of the gel [145]. It also serves to enhance the viscosity and viscoelastic moduli of the gel. As salinity increases or pH decreases, both the viscosity and viscoelastic moduli of the gel decrease. Brunauer-Emmett-Teller (BET) model and the radial-basis function artificial neural network model can be employed to determine the equilibrium adsorption capacity and the diffusion coefficient, two crucial parameters in the diffusion-based kinetic model [146]. In order to enhance system performance, it is more advantageous to focus on increasing the membrane moisture diffusivity rather than reducing the membrane heat conductivity. System performance is enhanced by a thinner membrane, although this may result in a slight increase in conductive heat loss [147]. Various studies have also endeavored to alter the membrane profile in order to enhance $\eta_d$ [148,149]. Greater curvature values lead to reduced permeability flux. When the curvature radius is reduced from 30 mm to 15 mm, $\eta_d$ of convex and concave membranes increases by 1.96 % and 1.74 %, respectively [149]. One potential approach to enhance the dehumidification efficiency of membranes involves altering the surface hydrophilicity through the application of additives or coatings [52].

Table 10 presents a comparison of the technical characteristics of various membrane dehumidification technologies, including membrane contactors, separation membranes, and absorption membranes. To eliminate the water vapor on the permeate side of the membrane and uphold the water vapor concentration, as depicted in Fig. 11.

Table 10. Comparative analysis of different membrane dehumidification technologies [52,139].

| Type | Membrane contactors | Separation membrane | Absorption membrane |
|---|---|---|---|
| Working principle | Surface absorption | Selective barrier | Absorption materials |
| Driving force and mechanism | Concentration gradient (liquid desiccant) | Pressure gradient transmembrane transport | Hydrophilic property of membrane materials |
| Key parameters | Mass transport resistance<br>Membrane wetting | $H_2O/N_2$ selectivity permeability<br>Solution diffusion | Ratio and capacity of absorption<br>Surface area |
| Physical structure | Porous, hydrophobicity, physical stability, high surface roughness, high membrane flux | Dense, hydrophilic or hydrophobic, physical stability, good mechanical performance | Nanofibers, hydrophily, physical stability, good mechanical performance, high surface roughness |
| Price | Low | Medium | High |
| Advantage | High membrane flux and $\eta_d$ | Modular design, high $\eta_d$, non-regeneration | High membrane flux |
| Disadvantage | Regeneration expensive<br>Porous membranes exist | High energy consumption<br>Low membrane flux | Less material selectivity<br>Significantly high price |

| Type | Membrane contactors | Separation membrane | Absorption membrane |
|---|---|---|---|
| | membrane wetting problems<br>Liquid transport | | |
| Application | Enthalpy exchanger | Accurate humidity control | Low energy and humidity |

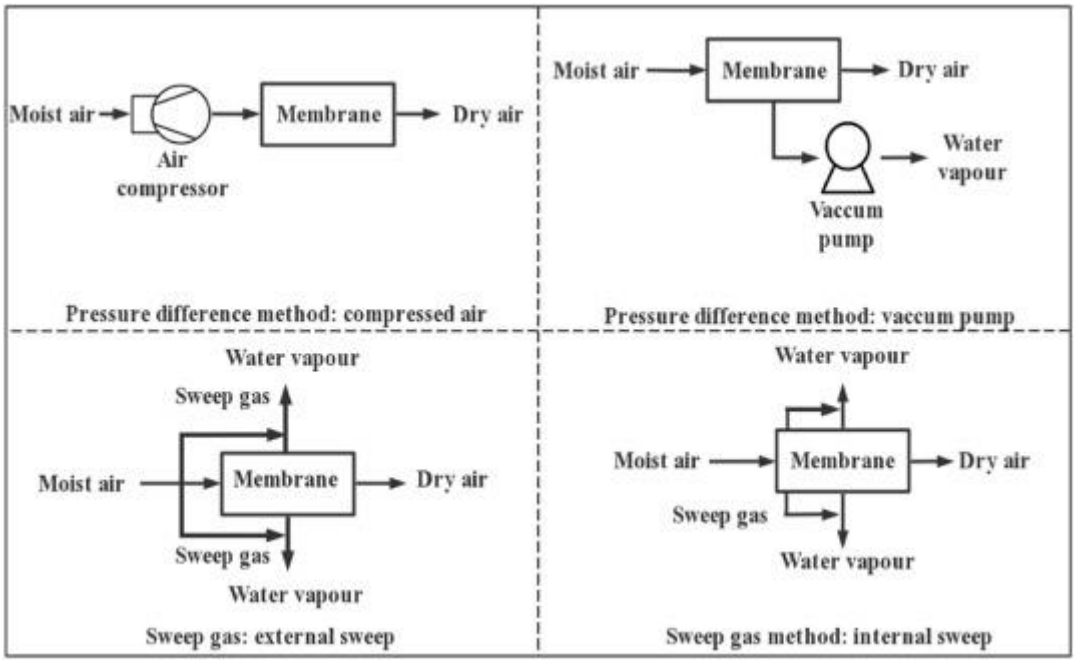


Fig. 11. Conceptual diagram of generation in membrane permeation process.

Employing the pressure difference method to elevate gas pressure necessitates greater membrane strength and increased pressure resistance in component equipment. When the operational pressure exceeds the pressure-bearing capacity of the membrane module, further increasing the working pressure will not enhance the adsorption capacity, but rather lead to damage of the membrane module. During the membrane dehumidification process, a thicker fouling layer necessitates a higher mechanical pressure. The dirt can only be removed when the pressure is sufficient. Two different methods for sweep gas can be utilized: external sweep gas and self-sweeping, which involves adjusting the membrane porosity. Increasing the flow rate of the sweep gas in a suitable manner has the potential to enhance the dehumidification performance [150]. The vacuum pumping method has extensive potential applications and has been one of the most researched methods [15]. However, vacuum pumps that operate between vacuum and atmospheric pressure require substantial energy consumption. This underscores the need for enhanced vacuum pump performance, careful pump selection, and integrated system design to minimize pump power usage. The influence of humidity on pressure reduction in a vacuum-pump system is less significant compared to the impact of temperature. As the vacuum pressure increases, the pressure decreases, leading to a reduction in the overall pumping power. For example, adjusting the vacuum pressure to a range of 0.66 kPa–2.66 kPa results in a nearly 11 % reduction in pressure drop at an air flow rate of 65 L/min [151]. Therefore, it is

possible to enhance dehumidification efficiency and decrease energy consumption by integrating the sweep gas with the vacuum pump [152,153].

Table 11 provides a comprehensive summary of membrane dehumidification systems. To achieve a more profound level of dehumidification, Petukhov et al. [154] were the first to employ chilled water for pre-dehumidification, followed by the use of a membrane contactor for additional dehumidification, resulting in a reduction of the air dew point temperature to −50 °C. The pre-dehumidification of outdoor air can be achieved by integrating membrane dehumidification technology with solid desiccants, followed by further dehumidification using the solid desiccants. This approach maximizes the membrane's dehumidification capacity in high humidity conditions and the solid desiccants' moisture adsorption capacity in low humidity conditions, rendering it appropriate for industrial environments with exceptionally low humidity levels.

Table 11. Summary of research on different membrane dehumidification systems.

| Membrane type | Dew point | Humidity ratio | Application | Results | Reference |
|---|---|---|---|---|---|
| A tetrafluoro-ethylene Teflon AF2400 composite plate membrane contactor (TEG solution) | −28 °C | 86 ppmv | Natural gas dehydration | Higher gas flow rate and pressure increase the transmembrane water flux | [155] |
| Porous polypropylene membrane contactor heat-exchanger with liquid coolant absorbent | −30 °C | 2.5 % wt | Pipeline transport of natural gas low-pressure pneumatic systems | −30 to −50 °C dew point<br>Heat consumption: 2.747 kW<br>Energy consumption: 1.31 kW | [154] |
| Polydimethylsiloxane and polyvinyltrimethylsilane nonporous flat membrane (TEG solution) | −30 °C | 0.24 g/kg | Removing carbon dioxide | $CO_2$ reduction: 10 times | [156] |
| Hollow fiber membranes | -8 to −13 °C | 0.01 vol% | Natural gas dehydration | Methane recovery: 98 %<br>Natural gas recovery: 97 % | [157] |
| Microporous polysulfone substrate plate membrane | −50 °C | 3.6 mg/cm$^3$ | Air Dehydration | Under 90 psig pressure operation | [158] |

### 3.5. Factors influencing deep dehumidification technology

As shown in Table 12, elevating the temperature and humidity of the incoming air results in higher humidity levels in the outgoing air and a reduction in dehumidification efficiency. The treatment of air is influenced by variations in environmental meteorological factors, and it is advisable to pre-treat outdoor air, such as through the use of pre-cooling equipment or heat exchangers. When utilizing a cooling apparatus, it is crucial to strike a balance between its cooling capacity and dehumidification effectiveness. Reducing the regeneration air temperature or enhancing the regeneration degree can also notably improve the performance of the dehumidification system [159]. Moderate temperatures for regeneration and air velocity have the potential to enhance COP of the system. An increase in air temperature, humidity, and cooling temperature results in a corresponding increase in COP. An optimal cycle time should be determined based on the experimental conditions and dehumidification capacity in order to achieve a higher COP.

Table 12. Operational parameters influencing dehumidification performance [160,161].

| Empty Cell | $t_{pin}$ ↑ | $_{dpin}$ ↑ | $_{mp}$ ↑ | **Cooling water temperature↑** | **Cooling water flow rate↑** | **Regeneration air temperature ↑** | **Regeneration air humidity ↑** | **Regeneration air flow rate↑** |
|---|---|---|---|---|---|---|---|---|
| $\eta_d$ | ↓ | ↓ | ↓ | ↓ | ↑ | ↓ | ↓ | ↑ |
| $d_{pout}$ | ↑ | ↑ | ↑ | ↑ | ↓ | ↓ | ↑ | ↓ |

## 4. Multifunctional development of dehumidification systems

### 4.1. Air humidification

Numerous studies have examined the humidification effects of dehumidification systems in arid winter regions with the aim of enhancing the utilization rate of dehumidification systems and transforming them into HVAC systems that can operate throughout the year [162]. By modifying the airflow direction and utilizing additional techniques, the system could potentially be utilized for indoor heating and humidification in the winter months. This not only resulted in a 10%–20 % improvement in thermal comfort [163,164] but also effectively decreased the spread of COVID-19 virus [165].

Cai et al. [166] proposed a heat pump liquid desiccant humidification and air conditioning system that incorporated a four-way valve for reversing the direction of refrigerant circulation. The system utilized a solution to absorb heat from the air and release moisture, thereby achieving both heating and humidification of the air. During the winter season, it was essential

to uphold the solution concentration within the range of 20 %–30 % to prevent freezing problems when outdoor temperatures fell below −15 °C. Substituting the solution with water was more susceptible to freezing [167]. Su et al. [168] introduced a frost-free air-source heat pump system that integrated membrane-based solutions. The dehumidifier was utilized to extract moisture from the air in order to mitigate the occurrence of frosting. The diluted solution underwent regeneration in a membrane regenerator before being utilized for air humidification, effectively addressing concerns related to droplet carryover and frosting. The solid desiccant wheel system provides benefits such as adiabatic humidification and prevents cross-contamination with fresh air, leading to its widespread application. Kawamoto et al. [169] introduced a desiccant wheel system integrated with a heat pump. The system has the capability to increase the humidity levels of outdoor air within the range of 1.8–2.3 g/kg up to 5.8 g/kg prior to its distribution into the indoor environment. Tu et al. [170] implemented a three-stage solid desiccant wheel humidification system. When employing two control strategies, the system was capable of fulfilling more than 96 % of the humidification needs in the cold and arid climate of Urumqi.

### 4.2. Water harvesting

In light of the global water crisis, there has been an increasing emphasis on the use of dehumidification systems for water collection, as noted in recent studies [171]. The collection of condensed water through condensation is a widely used method, and the quality of the resulting water can satisfy both industrial and household demands [165,172]. Zolfagharkhani et al. [173] employed condensation technology to generate around 26 L/day from ambient air, with an energy intensity of 300 Wh/L. However, the majority of solutions were not directly applicable for water collection. Efficient water harvesting often necessitates integration with other materials, such as zeolite, sand, and fabric, to enhance its effectiveness [174]. Solid desiccants have garnered greater interest in comparison to condensation water collection, owing to their superior water recovery efficiency and reduced energy consumption [175]. The water absorption capacities of various solid desiccant materials are depicted in Fig. 12. Kumar et al. [176] conducted a study on a solar-powered water collection system that utilized orange silica gel desiccant, resulting in the production of 0.98 L/day of drinking water. Gao et al. [177] investigated a new membrane-based water collection system, which, however, necessitated a relatively high air pressure. However, it is important to note that membrane water collection systems have limited applications because of their reduced airflow and consequently lower water collection rates [175]. Heidari et al. [178] introduced an air conditioning system that utilizes a silica gel desiccant wheel and an evaporative cooler to capture water condensation from the return air. The system produced 585 L of water in a week, of which around 296 L were utilized by the evaporative cooler, and the remaining 289 L were allocated for domestic hot water use. Tu and Hwang [179] presented a dehumidification water collection system that integrated a multi-stage desiccant wheel with a vapor compression cycle. Before entering the dehumidification process in the evaporator, the air was humidified by the multi-stage desiccant wheel in order to enhance water extraction. This approach has the potential to elevate the evaporation temperature and increase the rate of water collection.

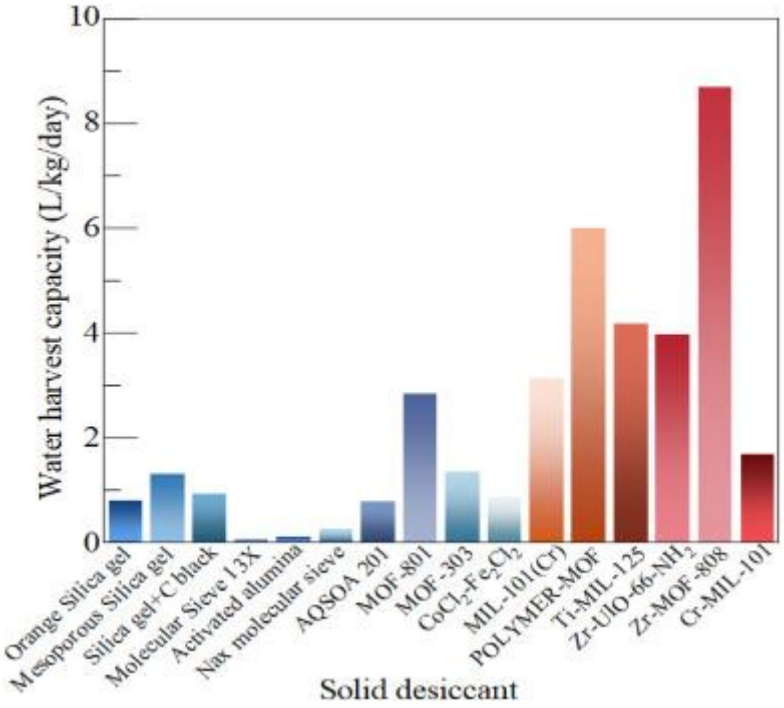


Fig. 12. Water harvesting capacity across different solid desiccant materials [181].

The humidification-dehumidification desalination technology plays a crucial role in water collection processes. It utilizes moving air as the medium for transporting water vapor. The warm air is subsequently channeled to the humidifier, where the evaporated seawater increases the moisture content of the air. Freshwater is acquired through the process of dehumidification using an apparatus. In contrast to a conventional direct-contact humidifier-based desalination facility, Tariq et al. [180] suggested the use of an air saturator for a humidification-dehumidification desalination system, which resulted in a 30 % increase in fresh water productivity, a 46 % improvement in recovery ratio, and an 11 % gain-output ratio. The newly implemented system demonstrated a 14 % reduction in cost per L compared to the conventional humidification-dehumidification desalination system, with a cost of 0.030 USD/L. It also exhibited a 7 % reduction in carbon footprint. The integration of humidification-dehumidification desalination systems with refrigeration, heat recovery, and renewable energy presents an effective approach for enhancing freshwater production and reducing operational expenses.

### 4.3. Air cleaning

The desiccants are responsible for extracting moisture and purifying volatile organic compounds, airborne particles, bacteria, and viruses within the air conditioning system [182]. As indicated in Table 13, the occurrence of droplet carryover in the hybrid air conditioning system using liquid desiccant dehumidification may result in a deterioration of indoor air quality, consequently affecting its viability for extensive residential use. However, research has indicated that the levels of bromide and lithium ions emitted into indoor air were found to be below the established air quality standards, thus not presenting any significant health risks [183]. However, the contentious elements of the dehumidification and purification system restricted its wider implementation. Conversely, membrane dehumidification systems largely

circumvent the aforementioned issues. Nevertheless, their manufacturing technologies are predominantly in the experimental phase, which impedes their widespread implementation [184].

Table 13. Air cleaning capacity across different dehumidification methods [185].

| Empty Cell | **Liquid desiccant** | **Soild desiccant** | **Condensation** |
|---|---|---|---|
| **Volatile organic compounds** | Removal | Removal | Non effect |
| **Bacteria** | Kill or deactivate | Non effect | Breed |
| **Particulates** | Capture | Release | Non effect |
| **Transfer carry** | Yes | No | No |

Rong et al. [186] conducted a study on the impact of silica gel desiccant wheel systems on three pollutants: toluene, carbon dioxide, and methane. The study revealed that the adsorption capacity for toluene was notably higher than that for carbon dioxide and methane. However, the adsorption capacity of silica gel desiccant for non-polar substances such as toluene and 1,2-dichloroethane was comparatively low [187]. Pang [188] suggested the utilization of MOF for the adsorption of indoor pollutants. At 25 °C, MIL-101 (Cr) exhibited a saturation purification capacity of 1027.091 mg/g for benzene and 592.701 mg/g for p-xylene, surpassing that of conventional materials by 2–5 times. However, its extensive use has not been realized because of its high expense. The dew point temperature ranges for different dehumidification technologies and various low-humidity industries are depicted in Fig. 13. In industries with low humidity, such as storage, food production, pharmaceutical manufacturing, precision instrument gas, and equipment purging, the necessary supply air dew point temperature ranges from 5 °C to −20 °C. The utilization of liquid desiccant technology and compressed air refrigeration dehumidification technology is commonly considered appropriate. For industries such as medical gas supply and fiber chemical production workshops, where the necessary supply air temperature ranges from −20 °C to −45 °C, membrane dehumidification technology or solid desiccant technology are commonly utilized [203]. In industries such as low-temperature industrial processes, semiconductor manufacturing, and aerospace, where the supply air temperature needs to be maintained below −40 °C, the preferred choice is usually solid desiccant technology or a combination of solid desiccant and compressed air dehumidification technology. In compact environments, such as precision manufacturing and power generation, solid desiccants packaged in a dry form are equipped with magnetic refrigeration and electric-driven dehumidification technologies, which are capable of fulfilling dehumidification requirements.

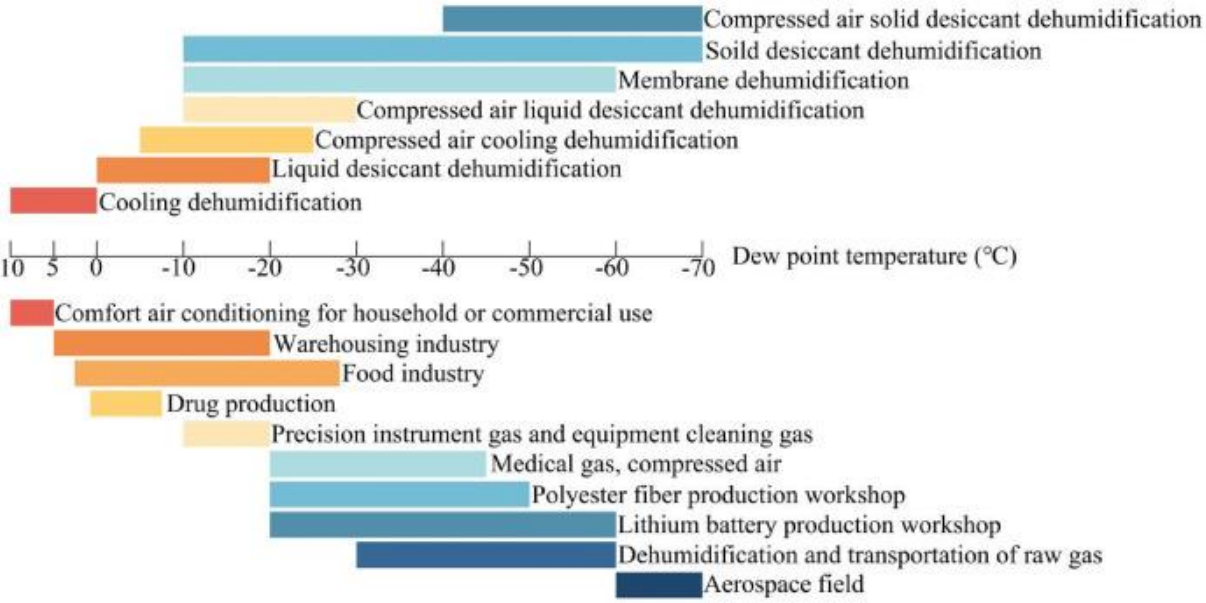


Fig. 13. Application range for different deep dehumidification systems in low-humidity industry.

### 4.4. Intelligent control and optimization

The intelligent control and optimization of dehumidification systems require the application of advanced techniques and algorithms for automated control and optimized adjustment. This is aimed at enhancing dehumidification performance and energy efficiency. As indicated in Table 14, the predominant focus of studies has been on the common methods of intelligent control and optimization as follows.

- (1)
  Establishment of predictive models contains predicting the response of the dehumidification system and using these predictions to optimize control.

- (2)
  Multi-objective optimization involves the optimization of the system with respect to objective functions such as operational expenses and dehumidification efficiency, while considering constraints such as load requirements and energy prices.

- (3)
  Artificial intelligence and machine learning facilitates the utilization of AI and machine learning methodologies. The system has the capability to acquire optimal control strategies by utilizing historical data and real-time feedback. The gradual improvement of system performance and energy efficiency is accomplished through an iterative process, which guarantees optimal operation [189,190].

Table 14. Summary of research on different optimization methods.

| Reference | Method | System description | Optimizing content | Results |
|---|---|---|---|---|
| [191] | Taguchi's method and genetic algorithm | Pressure-based molecular sieve bed | Adsorption uptake rate | Air pressure, air velocity, purge air flow rate affected the $R_d$ by 78.64 %, 0.41 %, and 17.38 % |
| [192] | Genetic algorithm and response surface method | Composite Hollow fiber Membrane | $R_d$ and dimensionless dehumidification amount per unit | Optimal conditions: air velocity is 0.18 m/s and water permeability is 5.1693 mol/($m^2$·Pa·s), filling rate is 0.17, fiber length is 30.19 cm, and fiber diameter is 0.6 mm |
| [193] | Particle swarm optimization algorithm | Hollow fiber membrane | Entropy generation and total annual cost | Most important factor: fiber inner diameter<br>Conflict between entropy generation and the total annual cost |
| [194] | Improved self-adaptive firefly algorithm | Solution cooling and dehumidification system | Energy efficiency, cooling and dehumidification performance | Reduced 12.49 % energy consumption<br>More suitable for high cooling and dehumidification load |
| [195] | Gene expression programming meta-model based fuzzy logic combined with genetic algorithm | Structured packed bed LiBr–$CaCl_2$ solution | Condensation rate , Moisture effectiveness, and latent heat factor | Air mass flux rate: 0.766 kg/$m^2$·s<br>Inlet air temperature: 30.745 °C<br>Solution flux rate: 1.812 kg/$m^2$·s<br>Air inlet humidity: 24 g/kg<br>Solution temperature: 24.01 °C<br>Total desiccant concentration: 48.1 % |
| [196] | Adaptive Neuro-Fuzzy inference system | Liquid desiccant with air conditioning | Energy efficiency | Average energy savings reached 9.5 %<br>Faster response |
| [197] | Response surface method and non-dominated sorted genetic algorithm II | Desiccant wheel of molecular sieve and silica gel | Operation of desiccant wheel | Surface area ratio effect on $d_{p,out}$: 37.11 % (silica gel) and 50.14 % (molecular sieve) |
| [198] | Adaptive Neuro Fuzzy Inference System and Artificial Neural Network | Liquid desiccant | High precision on the parameters | Solution temperature was the most important factors on the supply air temperature and humidity<br>Solution concentration was the most important factors on $\eta_d$ |

| Reference | Method | System description | Optimizing content | Results |
|---|---|---|---|---|
| [199] | Self-adaptive differential evolutionary algorithm | LiCl solution with air conditioning | Energy efficiency | Energy saved 22 % at morning, 16 % at afternoon and noon<br>Improve the energy efficiency with more regeneration air<br>Improve chiller COP with increasing chilled water and solution temperature |
| [200] | Proportional-control-technique-based new control strategy | Desiccant wheel with dew-point cooler | Energy consumption | Energy saved 40.9 % |
| [201] | Nondominated sort genetic algorithm-II | LiCl solution with absorption refrigeration and solar regeneration | Exergy destruction and cost rate | Exergy destruction rate: 50.99 kW<br>Cost rate: 1.60 $/h |

## 5. Analysis of deep dehumidification system

### 5.1. Application range of dehumidification system

For industries such as medical gas supply and fiber chemical production workshops, where the necessary supply air temperature ranges from −20 °C to −45 °C, membrane dehumidification technology or solid desiccant technology are commonly utilized [203]. In industries such as low-temperature industrial processes, semiconductor manufacturing, and aerospace, where the supply air temperature needs to be below −40 °C, solid desiccant technology or a combination of solid desiccant and compressed air dehumidification technology is commonly selected. In compact settings such as precision manufacturing and power generation, solid desiccants packaged in a dry form are equipped with magnetic refrigeration and electric-driven dehumidification technologies, which are capable of fulfilling the dehumidification requirements.

### 5.2. Energy analysis of dehumidification system

In engineering applications, it is imperative to not only consider the selection and design of various dehumidification technologies, but also to assess the trade-off between their energy performance and economic viability. Research on deep dehumidification systems has been diversified to account for various conditions, including architectural functions, operational conditions, and meteorological factors, resulting in different energy performances. The comparison of energy performance for dehumidification systems under various conditions is presented in Table 15.

Table 15. Summary of research on different deep dehumidification system.

| Reference | System description | Operation condition | System performance | System economy |
|---|---|---|---|---|
| [202] | Direct expansion air handling unit with LiBr solution | Outdoor: 33.5 °C, 19.5 g/kg<br>Indoor: 26 °C, 10.50 g/kg | $R_d$: 25.8 g/s<br>COPt: 4.13<br>COPt: 3.85 (electric chiller and boiler)<br>COPt: 2.98 (air source heat pump) | Re: 0.58 kW/kg<br>Dynamic payback period than electric chiller and boiler and air source heat pump were 0.9 years and 5.3 years |
| [203] | Liquid desiccant with mechanical vapor recompression | Outdoor:50 °C, 49.7 g/kg<br>Indoor: 100 °C, 12.4 g/kg | COPt: 4.45<br>Energy utilization ratio: 4.54<br>$R_d$ increased 18.5 % than heat pump | Re: 0.23 kWh/kg<br>Payback period: 1.54 years<br>Annual operational expense was decreased by 19.94 % to heat pump system |
| [204] | Cross flow $CaCl_2$ solution | Outdoor: 31 °C, 18 g/kg<br>Indoor: 27.8 °C, 12.5 g/kg | COPt: 0.86 | Payback period: 0.92 years<br>Operational expense saving was 31.4 % than vapor compression refrigeration system |
| [205] | KCOOH solution hybrid vapor compression | Outdoor:36 °C, 20 g/kg<br>Indoor: 29 °C, 15 g/kg | COPt: 2.5<br>COPt :1.72 (vapor compression regeriantion) | Payback period: 2.65 years<br>Annual year saved 212.9 $ |
| [206] | Solar energy with LiBr solution air conditioning | Outdoor: Hong Kong, China<br>Indoor: 24 °C, 10.24 g/kg | Chiller COP: 4.62<br>Chiller COP: 3.3 (vapor compressed refrigeration system) | Payback period:7 years<br>Energy savings for annual operation 6760 kWh |
| [207] | Desiccant wheel with air-conditioning | Outdoor: Beirut, Lebanon<br>Indoor: 24 °C, 10.89 g/kg | Cooling load: 9.2 kW–63.4 kW (conventional system)<br>7.4 kW–32.7 kW(hybrid system) | Payback period: 2–7 years (occupancy)<br>Downsizing system 20 %–48 % |

| Reference | System description | Operation condition | System performance | System economy |
|---|---|---|---|---|
| [208] | Ethaline desiccant air conditioning system | Outdoor: 26 °C, 14.79 g/kg~21.35 g/kg<br>Indoor: 26 °C, 10.5 g/kg | COPt: 1.406<br>Exergy efficiency: 32.65 % | Payback period: 37.5 years (2 kW), 14.8 years (20 kW), and 6.1 years (200 kW) |
| [209] | LiCl solution with vapor compression refrigeration system | Outdoor: Beijing, Shanghai, Nanjing<br>Indoor: cooling for data centers and supermarkets | COP of chiller increased 18.6 %<br>Exergy efficiency increased 27.9 % | Payback period: 2.4–3.2 years |
| [210] | Silica gel double-stage desiccant wheel for blast furnace | Outdoor: 32 °C, 18 g/kg<br>Indoor:57.2 °C, 9.92 g/kg | COP: 3.08<br>Average dehumidification capacity: 8.73 g/kg | Payback period: 0.55 years shorten than 1.64 year (LiBr adsorption refrigeration system) |
| [211] | Photovoltaic with LiCl double stage solution system | Outdoor: 30 °C, 19.26 g/kg<br>Indoor: 23.6 °C, 6.92 g/kg | COP of vapor compression chiller: 8.06 | Payback period: 7.51 years<br>Profit 5087 $/a<br>Power saving ratio: 55.65 % |
| [212] | Liquid air energy storage with air dehumidification and cooling system | Outdoor: 25 °C, 15.96 g/kg<br>Indoor:46 °C, 6.89 g/kg | System performance improved 11.7 % | Payback period: 11.5 years<br>System saved 9521 MWh/a |
| [213] | Solar regenerated $CaCl_2$ solution-microporous polypropylene membrane system | Outdoor: 31 °C, 19.15 g/kg<br>Indoor: 24 °C, 11.44 g/kg | The COP is higher than 3 (vapor compression refrigeration system) | Re: 0.3 kWh/kg<br>Payback period: 7.67 years |
| [214] | Solar regenerated $CaCl_2$ solution system | Outdoor: Beirut, Lebanon<br>Indoor: 25 °C, 10.89 g/kg | COP of desiccant unit: 0.41 (house) and 0.45 (restaurant) | Payback period: 11years<br>Operational expense saved 3819.1 $/a |
| [215] | MIL-100 (Fe) and conventional desiccant wheel | Outdoor: 30 °C, 21.57 g/kg<br>Regeneration temperature: 50 °C | COP and dehumidification capacity of MOFs wheel increases13%–19 % and 40%–48 % than conventional desiccant wheel | – |

| Reference | System description | Operation condition | System performance | System economy |
|---|---|---|---|---|
| [216] | MOFs coating heat exchanger system | Outdoor: 30 °C, 50 % RH<br>Indoor: 21 °C, 55 % RH | System COP:7.9 | Saving 36.1 % energy than vapor-compression air-conditioning |

While the dehumidification system varies, MOF-coated heat exchanger in the heat pump air conditioning system achieved the highest COP at 7.9. The liquid desiccant and vapor compression refrigeration system also achieved the highest COP of 4.45. Compared to the utilization of electric refrigeration, boilers, or air-source heat pumps, this system has demonstrated an increased COP of 7.2 % and 38.6 %, respectively [202]. Meanwhile, $R_d$ of a single heat pump dehumidification system was found to have increased. COP of the solid desiccant dehumidification system was low, with the desiccant wheel and high-temperature heat pump COP reaching only 4.11 [217]. Furthermore, the solar energy-regenerating desiccant system exhibited a higher COP. COP of a solar desiccant-evaporative cooling system has been reported to reach 25.5 in Darwin [218]. In the Australian region, the solar desiccant-evaporative cooling systems exhibited the highest COP, followed by hybrid solar desiccant-compression cooling systems or solar absorption cooling systems [218]. Incorporating a temperature range of 12–16 °C into HVAC system designs may be feasible in the future. HVAC system, equipped with desiccant dehumidification and a high-temperature chiller, is believed to possess a higher potential for energy conservation. A temperature increase of 1 °C in chilled water led to a 3 % rise in COP [219].

### 5.3. Economic analysis of dehumidification system

The initial investment is higher for the deep dehumidification system (e.g., dehumidifier, regenerator, and heater) compared to a compressed vapor refrigerant system due to the additional devices. The economic comparison of deep dehumidification systems under various conditions is presented in Table 15. In the Mediterranean region of Boulder, typical commercial buildings experienced a 30 % reduction in $C_e$ of dehumidification systems when compared to traditional air conditioning systems [220]. However, in Beijing, a temperate region, and Los Angeles, also a temperate region, researchers observed that the electricity consumption of liquid desiccant dehumidification systems was 20%–30 % higher than that of air-conditioning systems lacking dehumidifiers. As depicted in Fig. 14, the solution dehumidification and membrane dehumidification systems, equipped with heat exchangers and cooling units, exhibited the lowest $R_e$ values, predominantly falling within the range of 0.23–0.58. The utilization of renewable energy, waste heat, and other resources for the regeneration of desiccants can additionally decrease $R_e$. In terms of payback, the implementation of a dehumidification system also yielded the most rapid return on investment. The minimum payback period for investment may be less than 1 year [204]. In contrast to these systems, solid desiccant dehumidification

systems were more suitable for large industrial sites because of their size, resulting in a shorter investment payback period. The integration of heat pumps and solar energy equipment has led to an increase in the initial investment required for dehumidification systems, resulting in many systems having a payback period exceeding 10 years. The solar thermal system paired with a natural gas boiler demonstrated a shorter payback period, whereas the solar thermal system combined with an electric heat pump exhibited a longer payback period [221]. In order to evaluate the economic viability, it is essential to comprehensively evaluate the operational expenses, initial capital outlay, and the life cycle (10–15 years) to ascertain the feasibility of the economy.

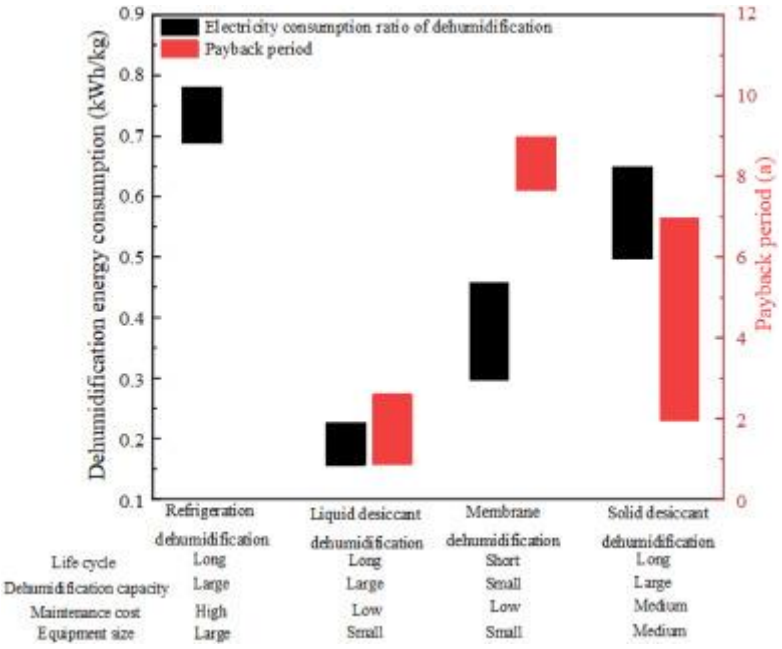


Fig. 14. Energy efficiency and economic analysis of different dehumidification systems.

### 5.4. Environmental analysis of dehumidification system

The incorporation of a desiccant unit into the air conditioning system led to an enhanced energy efficiency ratio for the chiller, as it was only required to handle sensible loads. If the energy efficiency ratio increased from 2.2 to 2.7 (a 23 % increase), the corresponding decrease in $CO_2$ equivalent emissions would be approximately 7 %. The primary rationale for decreasing $CO_2$ emissions in desiccant dehumidification systems is their lower energy consumption in comparison to conventional air conditioning systems. This led to a decrease in the use of fossil fuels for electricity generation, resulting in the avoidance of $CO_2$, $SO_2$, $NO_2$, and CO emissions. The reduction of $CO_2$ emissions was significantly influenced by the carbon emission factor of electricity [190,222]. The desiccant system was only effective in reducing $CO_2$ emissions when

$CO_2$ emission factor exceeded 0.40 kg $CO_2$/kWh to 0.50 kg $CO_2$/kWh. In Poland, the greatest reduction in carbon emissions, exceeding 50 %, was attained due to a $CO_2$ emissions factor of 1.19 kg $CO_2$/kWh.

Life cycle assessment (LCA) is a systematic approach utilized to assess the environmental impact of material acquisition, manufacturing, usage, including assembly, usage, and maintenance, as well as the end-of-life stage, considering assembly and disposal in dehumidification systems. Kabeel and Bassuoni [223] employed a LCA methodology to examine liquid desiccant hybrid-air conditioning systems and conventional vapor compression systems over a 20-year period with a 95 % recycle rate. The study revealed that energy usage and $CO_2$ emissions constitute approximately 95 % of the total impact of the desiccant dehumidifier. The energy consumption of the conventional system exceeded that of the desiccant hybrid air conditioning system, primarily because the compressor consumption was higher than the heater consumption. Ortis and Khatiwada [224] employed a LCA methodology to examine two desiccant wheel systems with a 10-year lifespan. A system was characterized by a 2700 $m^3$/h air flow rate and a weight of 370 kg, while B system featured a 14,000 $m^3$/h air flow rate and a weight of 3.3 tonnes, inclusive of an extra pre-cooler. The study revealed that steel is the predominant material in two systems for material acquisition and manufacturing, constituting 88 % in system A and 50 % in system B, respectively. The operational stage exerted the most significant impact (74%–99 %) on the entire life cycle, primarily attributable to the continuous demand for electricity. The impacts of transportation and the end-of-life stage should not be disregarded. In subsequent LCA studies, the calculation can incorporate reductions in water collection and humidification emissions.

## 6. Conclusions

This study provides a comprehensive review of the deep dehumidification system, focusing on its applications in low-humidity environments. A variety of desiccant materials, components, and system configurations are presented. These characteristics were elucidated with regard to adsorption, water harvesting capacity, and heat transfer efficiency. The review centered on examining the effects of dehumidification performance, energy performance, economic feasibility, and environmental impact. The primary findings can be summarized as follows.

(1) This study employed a matching analysis to assess the suitability of dehumidification technology for various humidity field requirements. The dew point temperature of the supply air provided by the liquid desiccant system ranges from −20 °C to 0 °C, thereby satisfying the humidity needs of cold storage, pharmaceutical production, and industrial sectors. The dew point temperature of the supply air provided by the solid desiccant system ranges from −70 °C to −10 °C, making it suitable for ultra-low humidity applications such as semiconductor manufacturing and raw material drying. The integration of dehumidification systems with compressed air and refrigeration technology has the potential to further reduce the dew point temperature.

(2) Zeolites and molecular sieves exhibit the highest adsorption capacity among solid desiccants; however, their regeneration temperature can reach as high as 250 °C. MOFs are considered to be the next generation of advanced materials due to their customizable

structures, exceptional structural integrity, remarkable hydrophilicity, and unique host-guest interactions, making them suitable for specific applications. Desiccant cooling heat exchange is a widely utilized method in building applications and exhibits a high COP when integrated with air conditioning systems, owing to its capacity for direct regeneration through condensation heat. The adsorption bed and dehumidification wheel are frequently utilized in the industrial sector, and employing multi-stage desiccant wheels and internal cooling are effective approaches for lowering the regeneration temperature.

(3) The vapor pressure is indicative of the dehumidification capabilities of liquid desiccants, with LiCl and LiBr solutions demonstrating high performance in this regard. The liquid desiccant air ratio, flow pattern, and mass transfer correlations are crucial elements to consider when analyzing liquid dehumidification systems. The size of the equipment and the efficiency of dehumidification are significantly influenced by the ratio of liquid desiccant-to-air flow rate. The efficiency of the counterflow module is notably high; however, further detailed information is required regarding the interaction between droplets and air. Considering unstable droplet and air mass transfer processes and optimizing assumptions can contribute to the development of more dependable predictive models. The addition of surfactants or the application of nanoparticles to hydraulic materials has been found to be effective in improving heat and mass transfer. Multi-stage solution dehumidifiers and internal cooling systems can effectively harness low-grade heat sources to regenerate liquid dehumidification systems. Liquid desiccant systems exhibiting higher COP and shorter investment payback periods are suitable for application in both building and industrial settings.

(4) The membrane dehumidification technology effectively addresses the issue of droplet carryover in solution dehumidification technology. The membrane contactor represents the most advanced technology in this field. Current research is centered on the development of membrane materials in order to achieve improved performance parameters. However, the high cost of membrane materials has led current research to predominantly concentrate on numerical simulations and small-scale laboratory experiments, necessitating further validation for practical engineering applications.

(5) The integration of refrigeration technology with renewable energy and waste heat sources has the potential to significantly enhance COP of dehumidification systems. The combination of local energy policy subsidies and carbon prices, along with the implementation of renewable energy dehumidification systems, has the potential to significantly reduce the investment payback period. To address year-round utilization and future development demands, dehumidification systems have evolved to incorporate air humidification, water collection, and air purification functions. The advancement of multifunctional systems in upcoming applications has the potential to mitigate a portion of carbon emissions across the entire lifecycle.

(6) Dehumidification-hybrid air conditioning systems yield substantial carbon reductions in comparison to traditional air conditioning systems. In the lifecycle assessment analysis, the carbon emissions during the operational phase of the dehumidification-coupled air conditioning system may constitute as much as 95 % of

the total emissions. The reduction of $CO_2$ emissions is significantly influenced by the carbon emission factor of electricity. The impacts of transportation and the end-of-life stage should not be disregarded.

## 7. Recommendations for future work

Significant research areas in deep dehumidification technology persist, encompassing materials, components, and systems. The primary areas for future research are outlined as follows.

(1)Further research and development are needed to create desiccant materials that are both efficient and cost-effective, capable of meeting humidity requirements in a variety of application conditions.
(2)The optimization of operating parameters and key equipment involves finding the optimal balance between regenerator and dehumidifier side flow rates, as well as enhancing heat and mass transfer between desiccants and gas phases.

(3)The optimization of cooling and heating sources, combined with renewable energy systems, aims to improve the utilization of low-grade heat sources and facilitate energy recovery. Current research is focused on addressing the high energy consumption associated with regeneration in order to achieve efficient regeneration of desiccant materials.
(4)The investigation of the integration of various dehumidification technologies represents a future trend in development. Further research is required for emerging dehumidification technologies, such as electrodialysis dehumidification and high-voltage discharge dehumidification, to be applicable for deep dehumidification in precision manufacturing and confined spaces.

## Funding

This work was supported by the Fundamental Research Funds for Beijing University of Civil Engineering and Architecture. And sponsored by the Beijing University of Civil Engineering and Architecture Post Graduate Innovation Project [DG2023010].

## Declaration of competing interest

The authors declared that they have no conflicts of interest to this work.

## Acknowledgments

The images in this research have been copyrighted. We thank the reviewers and editors of Renewable and Sustainable Energy Reviews for their advice.

## Data availability

No data was used for the research described in the article.

## References

[1] Indrawan W, Lubis A, Nasruddin, Alhamid MI. The experimental study of dehumidification and regeneration processes in a fin and tube liquid desiccant system. Case Stud Therm Eng 2022/11/01/2022;39:102440.
[2] Woods J, et al. Humidity's impact on greenhouse gas emissions from air conditioning. Joule 2022;6(4):726–41. 2022/04/20/.
[3] Yin H, Yin Y. Current status and development trend of dehumidification technology in low-humidity industries. 2022.
[4] Ahmed S, Nelson PA, Dees DW. Study of a dry room in a battery manufacturing plant using a process model. J Power Sources 2016;326:490–7.
[5] Climatronics. Humidity control in food industry. DEC.28,2020. https://www.climatronics.in/humidity-control-in-food-industry/.
[6] Phymetrix. 2016. https://www.phymetrix.com/industries-applications/natural-gas/#1609802371904-b87f2ab0-71fa). Natural Gas Applications.
[7] Yusheng L. Purification technology (dalian) Co. May.20, 2023. https://www.antpedia.com/ibook8960/s/21154-s.html).Applicationofmodularadsorptiondryerinmedicalcompressedairsystem.
[8] Denmark CA Si. Managing humidity in cold store installations. NOV.25, 2021. https://www.klimavex.sk/public/files/COTES/KTL-C-MANAGE_HUMIDITY_COLDSTORE-EN.pdf.
[9] Shamim JA, Hsu W-L, Paul S, Yu L, Daiguji H. A review of solid desiccant dehumidifiers: current status and near-term development goals in the context of net zero energy buildings. Renew Sustain Energy Rev 2021;137:110456. 2021/03/01/.
[10] Jani DB, Mishra M, Sahoo PK. A critical review on application of solar energy as renewable regeneration heat source in solid desiccant – vapor compression hybrid cooling system. J Build Eng 2018;18:107–24. 2018/07/01/.
[11] Gao DC, Sun YJ, Ma Z, Ren H. A review on integration and design of desiccant airconditioning systems for overall performance improvements. Renew Sustain Energy Rev 2021;141:110809. 2021/05/01/.
[12] Abd-Elhady MM, Salem MS, Hamed AM, El-Sharkawy II. Solid desiccant-based dehumidification systems: a critical review on configurations, techniques, and current trends. Int J Refrig 2022;133:337–52. 2022/01/01/.
[13] Wen T, Lu L. A review of correlations and enhancement approaches for heat and mass transfer in liquid desiccant dehumidification system. Appl Energy 2019;239:757–84. 2019/04/01/.
[14] Qi R, Dong C, Zhang L-Z. A review of liquid desiccant air dehumidification: from system to material manipulations. Energy Build 2020;215:109897. 2020/05/15/.
[15] Qu M, Abdelaziz O, Gao Z, Yin H. Isothermal membrane-based air

dehumidification: a comprehensive review. Renew Sustain Energy Rev 2018;82: 4060–9.
[16] Aljerf L. Reduction of gas emission resulting from thermal ceramic manufacturing processes through development of industrial conditions 2016;17:1–10.
[17] Fang S, et al. Cascade deep air dehumidification with integrated direct-contact cooling and liquid desiccant absorption. Energy Convers Manag 2022;268: 115959. 2022/09/15/.
[18] Su JJ, Hongguang. Feasibility of a two-stage liquid desiccant dehumidification system driven by low-temperature heat and power. Appl Therm Eng: Design, processes, equipment, economics 2018;128.
[19] Guan B, Liu X, Zhang T. Modification of analytical solutions of coupled heat and mass transfer processes in liquid desiccant dehumidifier for deep dehumidification. Int J Heat Mass Tran 2020;165.
[20] Evron Y, Gommed K, Grossman G. Efficient deep dehumidification hybrid air conditioning system. 2019. p. 50–8.
[21] Cao BW, Yin YG, Zhang F, Ji Q, Chen WH. Liquid desiccant-based deep dehumidifier working with a novel ionic liquid: prediction model and performance comparison. Int J Refrig Feb 2023;146:74–87.
[22] Guan B, Zhang T, Liu X. On-site performance investigation of a desiccant wheel deep- dehumidification system applied in lithium battery manufacturing plant. Energy Build 2021;232.
[23] Guan BW, Liu XH, Zhang T. On the importance of air-solution flow rate matching in liquid-desiccant deep-dehumidification system. Int J Heat Mass Tran Jan 2021; 164:120614.
[24] Guan BW, Liu XH, Zhang T, Ma ZY, Chen LL, Chen XY. Experimental and numerical investigation of a novel hybrid deep-dehumidification system using liquid desiccant. Energy Convers Manag Jul 2019;192:396–411.
[25] Guan BW, Zhang T, Jun L, Liu XH. Exergy analysis and performance improvement of liquid-desiccant deep-dehumidification system: an engineering case study. Energy Apr 2020;196:117122.
[26] Tu R., Hwang Y., Cao T., Hou M., Xiao H. Investigation of adsorption isotherms and rotational speeds for low temperature regeneration of desiccant wheel systems. Int J Refrig 2017;86:495-509.
[27] Ruixuan Z, Chengchu Y, Mei L. Dehumidification classification and advanced research in deep dehumidification technology. Journal of Refrigeration 2020;41 (6):12–21 (in Chinese).
[28] Zhang M, Huang S, Li P, Shah KW, Zhang X. Application of dehumidification as anti-corrosion technology on suspension bridges: a review. Appl Therm Eng 2021; 199:117549.
[29] KELIN. Water cooling refrigerated Air Dryer for centrifugal compressor. http ://www.china-air-dryer.com/pid18224150/200Nm3-min-water-cooling-refriger ated-Air-Dryer-for-centrifugal-compressor.htm; 2023.
[30] Yang S, Deng C, Liu Z. Optimal design and analysis of a cascade LiBr/H2O absorption refrigeration/transcritical CO2 process for low-grade waste heat

recovery. Energy Convers Manag 2019;192:232–42. 2019/07/15/.
[31] Sun J, Ge Z, Fu L. Investigation on LiBr-H2O double evaporation-absorption heat pump (DEAHP) for heat recovery under lower driving sources. Appl Therm Eng 2017;125:978–85. 2017/10/01/.
[32] Corporation M. The dehumidification handbook. third ed. 2019. Copyright 1989, 2002 and 2019.ISBN 0-9717887-0-7.
[33] Azizi HR, Pakdehi SG, Babaee S. Thermodynamic study and optimization a nanozeolite for dehydration liquid fuel (DMAZ) using taguchi L_(16) orthogonal array. Arabian J Sci Eng 2018;43(5):2465–72.
[34] Yamamoto S, Araki K, Moriguchi S, Miyazawa H, Suzuki T. Effects of wetness and humidity on transonic compressor of gas turbine. Int J Heat Mass Tran 2021;178 (2):121649.
[35] Chen JJ. Electrothermal desiccant regeneration technique for air dehumidification. Processes 2021;9.
[36] Zhang P, Bu X, Yang Y. Technical-economic evaluation of an energy-integrated temperature swing adsorption process for compressed air drying. Comput Chem Eng: An International Journal of Computer Applications in Chemical Engineering 2022;157.
[37] Fang S. Study on a deep dehumidification system using liquid desiccant driven by compression heat of air separation units. Professor PHD dissertation. China: School of Energy Engineering, Zhejiang University; 2022.
[38] Huang J, Xu Y, Guo H, Geng X, Chen H. Dynamic performance and control scheme of variable-speed compressed air energy storage. Appl Energy 2022;325: 119338. 2022/11/01/.
[39] Guo H, Xu Y, Zhang X, Liang Q, Wang S, Chen H. Dynamic characteristics and control of supercritical compressed air energy storage systems. Appl Energy 2021; 283:116294. 2021/02/01/.
[40] Qianyilang Q, Nobunaga O. Dehumidification design. China Architecture & Building Press; 1983.
[41] Zhan C, Yin Y, Guo X, Jin X, Zhang X. Investigation on drying performance and alternative analysis of different liquid desiccants in compressed air drying system. Energy 2018;165.
[42] Bhowmik M, Muthukumar P, Anandalakshmi R. Experimental study of coupled heat and mass transfer phenomena between air and desiccant in a solar assisted thermal liquid desiccant system. Int J Therm Sci 2021;162:106795. 2021/04/01/
.
[43] Fang S, et al. High-performance multi-stage internally-cooled liquid desiccant dehumidifier for high gas–liquid flow ratios. Energy Convers Manag 2021;250: 114869. 2021/12/15/.
[44] Naik BK, Muthukumar P. Experimental investigation and parametric studies on structured packing chamber based liquid desiccant dehumidification and regeneration systems. Build Environ 2019;149:330–48. 2019/02/01/.
[45] Qi R, Dong C, Zhang L-Z. Development of liquid-air mass transfer correlations for liquid desiccant dehumidification considering the liquid/air contact and film

instability. Int J Heat Mass Tran 2019;141:491–502. 2019/10/01/.
[46] Fekadu G, Subudhi S. Renewable energy for liquid desiccants air conditioning system: a review. Renew Sustain Energy Rev 2018;93:364–79.
[47] Yin Y, Zheng B, Yang C, Zhang X. A proposed compressed air drying method using pressurized liquid desiccant and experimental verification. Appl Energy 2015;141 (mar.1):80–9.
[48] Kashif SM, Ding Y, Li Q, Xuan Y, Gao N, Chen G. Novel multifunctional open absorption heat pump system with compressed air dryer assisted preliminary flash regeneration-An industrial application. Appl Therm Eng: Design, processes, equipment, economics 2022;211:211.
[49] Han Y, Liao J, Li W, Ma H, Bai Z. Insight into the interaction between hydrogen bonds in brown coal and water. Fuel 2019;236:1334–44. 2019/01/15/.
[50] Wang Z, Orejon D, Sefiane K, Takata Y. Coupled thermal transport and mass diffusion during vapor absorption into hygroscopic liquid desiccant droplets. Int J Heat Mass Tran 2019;134:1014–23. 2019/05/01/.
[51] Liu X, Qu M, Liu X, Wang L. Membrane-based liquid desiccant air dehumidification: a comprehensive review on materials, components, systems and performances. Renew Sustain Energy Rev 2019;110(AUG):444–66.
[52] Lim H, Goh K, Tian M, Wang R. Membrane-based air dehumidification: a comparative review on membrane contactors, separative membranes and adsorptive membranes. Chin J Chem Eng 2022;41:121–44. 2022/01/01/.
[53] Salikandi M, Ranjbar B, Shirkhan E, Priya SS, Sudhakar K. Recent trends in liquid desiccant materials and cooling systems: application, performance and regeneration characteristics. J Build Eng 2020;33:101579.
[54] Koronaki IP, Christodoulaki RI, Papaefthimiou VD, Rogdakis ED. Thermodynamic analysis of a counter flow adiabatic dehumidifier with different liquid desiccant materials. Appl Therm Eng 2013;50(1):361–73.
[55] Liu XH, Yi XQ, Jiang Y. Mass transfer performance comparison of two commonly used liquid desiccants: LiBr and LiCl aqueous solutions. Energy Convers Manag 2011;52(1):180–90.
[56] Ren H, Ma Z, Gschwander S. Characterisation and evaluation of a new phase change enhanced working solution for liquid desiccant cooling systems. Appl Therm Eng 2019;150:1197–205. 2019/03/05/.
[57] Bai H, Zhu J, Chu J, Chen X, Cui Y, Yan Y. Influences of the mixed LiCl-CaCl_2 liquid desiccant solution on a membrane-based dehumidiflcation system: parametric analysis and mixing ratio selection. Energy Build 2019;183(JAN): 592–606.
[58] Wen T, Luo Y, Sheng L. Experimental study on the corrosion behavior and regeneration performance of KCOOH aqueous solution. Sol Energy 2020;201: 638–48.
[59] Li XW, Zhang XS, Wang G, Cao RQ. Research on ratio selection of a mixed liquid desiccant: mixed LiCl– CaCl2 solution. Sol Energy 2008;82(12):1161–71.
[60] Zhao X, Li X, Zhang X. Selection of optimal mixed liquid desiccants and performance analysis of the liquid desiccant cooling system. Appl Therm Eng

2015;94:622–34.
[61] Li SMH. Vapour pressures, densities, and viscosities of the aqueous solutions containing (triethylene glycol or propylene glycol) and (LiCl or LiBr). J Chem Therm 2009;41:623-631.
[62] Guo Y, Ma Z, Al-Jubainawi A, Cooper P, Nghiem LD. Using electrodialysis for regeneration of aqueous lithium chloride solution in liquid desiccant air conditioning systems. Energy Build 2016;116:285–95.
[63] Luo Y, Shao S, Xu H, Tian C. Dehumidification performance of [EMIM]BF4. Appl Therm Eng 2011;31(14–15):2772–7.
[64] Li, et al. Vapor pressure measurement of the ternary systems H2O + LiBr + [dmim]Cl, H2O + LiBr + [dmim]BF4, H2O + LiCl + [dmim]Cl, and H2O + LiCl + [dmim]BF4. J Chem Eng Data 2011;56(1):97–101.
[65] Watanabe H, et al. Design of ionic liquids as liquid desiccant for an air conditioning system. Green Energy Environ 2019;4(2):139–45. 2019/04/01/.
[66] Dong C, Lu L, Qi R. Model development of heat/mass transfer for internally cooled dehumidifier concerning liquid film shrinkage shape and contact angles. Build Environ 2017;114:11–22. 2017/03/01/.
[67] Wen, Tao, Lu, Lin, Dong, Chuanshuai. Enhancing the dehumidification performance of LiCl solution with surfactant PVP-K30. Energy Build 2018;171: 183-195.
[68] Wen T, Lu L, Dong C, Luo Y. Investigation on the regeneration performance of liquid desiccant by adding surfactant PVP-K30. Int J Heat Mass Tran 2018;123 (aug):445–54.
[69] Dong C, Lu L, Wen T. Experimental study on dehumidification performance enhancement by TiO2 superhydrophilic coating for liquid desiccant plate dehumidifiers. Build Environ 2017;124(nov):219–31.
[70] Yang L, Du K, Niu XF, Cheng B, Jiang YF. Experimental study on enhancement of ammonia–water falling film absorption by adding nano-particles. Int J Refrig 2011;34(3):640–7. 2011/05/01/.
[71] Wen T, Lu L, Zhong H. Investigation on the dehumidification performance of LiCl/H 2 O-MWNTs nanofluid in a falling film dehumidifier. Build Environ 2018; 139(JUL):8–16.
[72] Wen T, Lu L, Zhong H, Dong C. Experimental and numerical study on the regeneration performance of LiCl solution with surfactant and nanoparticles. Int J Heat Mass Tran 2018;127(PT.B):154–64.
[73] Wang, et al. Study on an internally-cooled liquid desiccant dehumidifier with CFD model. Appl Energy 2017;194:399-409.
[74] Chen Y, Zhang X, Yin Y. Experimental and theoretical analysis of liquid desiccant dehumidification process based on an advanced hybrid air-conditioning system. Appl Therm Eng 2016;98:387–99.
[75] Guan B, Liu X, Zhang T. Analytical solutions for the optimal cooling and heating source temperatures in liquid desiccant air-conditioning system based on exergy analysis. Energy 2020:117860.
[76] Zhang L, Song X, Zhang X. Analysis and optimization of total heat recovery

devices by using liquid desiccant as a coupling fluid in air-conditioning systems. Energy Build 2018;172:493-504.
[77] Giampieri A, Ma Z, Smallbone A, Roskilly AP. Thermodynamics and economics of liquid desiccants for heating, ventilation and air-conditioning – an overview. Appl Energy 2018;220:455–79.
[78] Wen T, Luo Y, He W, Gang W, Sheng L. Development of a novel quasi-3D model to investigate the performance of a falling film dehumidifier with CFD technology. Int J Heat Mass Tran 2019;132:431–42. 2019/04/01/.
[79] Wen T, Wang M, Chen Y, He W, Luo Y. Thermal properties study and performance investigation of potassium formate solution in a falling film dehumidifier/regenerator. Int J Heat Mass Tran 2019;134:131–42. 2019/05/01/.
[80] Moulinkumar Shah N, Mehta JR, Sharma S. Parametric investigations on a novel bubble column liquid desiccant dehumidifier with internal cooling. Energy Build 2023;285:112913. 2023/04/15/.
[81] Lun W, Li K, Liu B, Zhang H, Yang Y, Yang C. Experimental analysis of a novel internally-cooled dehumidifier with self-cooled liquid desiccant. Build Environ 2018;(Aug):141.
[82] Yang Z, Zhang K, Hwang Y, Lian Z. Performance investigation on the ultrasonic atomization liquid desiccant regeneration system. Appl Energy 2016;171:12–25. 2016/06/01/.
[83] Yang Z, Chen L-A, Tao R, Zhong K. Determination of cost-efficient cooling power range for improving the performance of internally cooled ultrasonic atomization liquid desiccant dehumidifiers. Indoor Built Environ 2020;29(9):1260–76.
[84] Kashif Shahzad M, Ding Y, Xuan Y, Gao N, Chen G. Performance analysis of a novel double stage multifunctional open absorption heat pump system: an industrial moist flue gas heat recovery application. Energy Convers Manag 2022;254:115224. 2022/02/15/.
[85] Peng D, Cao Z. Modeling and performance analysis of a hybrid-connected twostage liquid dehumidification fresh air system based on CaCl2/LiCl double solution. Appl Therm Eng 2021;199:117529.
[86] Park J-Y, Dong H-W, Cho H-J, Jeong J-W. Energy benefit of a cascade liquid desiccant dehumidification in a desiccant and evaporative cooling-assisted building air-conditioning system. Appl Therm Eng 2019;147:291–301. 2019/01/25/.
[87] Su B, Han W, Sui J, Jin H. A novel liquid desiccant dehumidification system driven by low-temperature heat for industrial application. Energy Proc 2017;105:1953–9.
[88] Aljerf L. High-efficiency extraction of bromocresol purple dye and heavy metals as chromium from industrial effluent by adsorption onto a modified surface of zeolite: kinetics and equilibrium study. J Environ Manag 2018;225:120–32. 2018/11//.
[89] Karmakar A, Prabakaran V, Zhao D, Chua KJ. A review of metal-organic frameworks (MOFs) as energy-efficient desiccants for adsorption driven heattransformation applications. Appl Energy 2020;269.

[90] Wang C, Yang B, Ji X, Zhang R, Wu H. Study on activated carbon/silica gel/ lithium chloride composite desiccant for solid dehumidification. Energy 2022; (Jul.15):251.
[91] Lizhi Z. Dehumidification technology. Beijing, China: Chemical Industry Press; 2004.
[92] Eicker U, et al. Experimental investigations on desiccant wheels. Appl Therm Eng 2012;42:71–80. none.
[93] Zendehboudi A, Angrisani G, Li X. Parametric studies of silica gel and molecular sieve desiccant wheels: experimental and modeling approaches. Int Commun Heat Mass Tran 2018;91:176–86.
[94] Rippy KC, Volk E, Beers R, Kozubal E, Gauderman K, Vidal J. Corrosion of metal alloys in potassium acetate solutions for liquid desiccant dehumidification and air conditioning. Energies 2022;15.
[95] Andres, et al. Experimental investigation on performance of a novel composite desiccant coated heat exchanger in summer and winter seasons. Energy 2019; 166:506–18.
[96] Ge TS, Zhang JY, Dai YJ, Wang RZ. Experimental study on performance of silica gel and potassium formate composite desiccant coated heat exchanger. Energy 2017;141(PT.1):149–58.
[97] Wang W, Wu L, Li Z, Fang Y, Ding J, Xiao J. An overview of adsorbents in the rotary desiccant dehumidifier for air dehumidification. Dry Technol 2013;31(12): 1334–45.
[98] Lin L, Zhao-hong H, Jie-chao C, Li-sheng D, Noriyuki K, Hong-yu H. Development on solid composite desiccants forDesiccant cooling systems. Advances in New and Renewable Energy 2017;5(5):9.
[99] Zheng J, et al. Pore-engineered metal–organic frameworks with excellent adsorption of water and fluorocarbon refrigerant for cooling applications. J Am Chem Soc 2017;139(31):10601–4.
[100] Zeng Y, Woods J, Cui S. The energy saving potential of thermo-responsive desiccants for air dehumidification. Energy Convers Manag 2021;244:114520.
[101] Development of solid super desiccants based on a polymeric superabsorbent hydrogel composite. RSC Adv 2015;5(73):59583–90.
[102] Vivekh P, Kumja M, Bui DT, Chua KJ. Recent developments in solid desiccant coated heat exchangers – a review - ScienceDirect. Appl Energy 2018;229: 778–803.
[103] Lee J, Lee DY. Sorption characteristics of a novel polymeric desiccant. Int J Refrig 2012;35(7):1940–9.
[104] Dai M, et al. A nanostructured moisture-absorbing gel for fast and large-scale passive dehumidification. Adv Mater 2022;34(17):2200865.
[105] Vivekh P, Islam MR, Chua KJ. Experimental performance evaluation of a composite superabsorbent polymer coated heat exchanger based air dehumidification system. Appl Energy 2020;260.
[106] C. A. B. F, et al. Development of biomass based-activated carbon for adsorption dehumidification - ScienceDirect. 2021.

[107] Lee JG, Bae KJ, Kwon OK. Experimental investigation of the solid desiccant dehumidification system with metal organic frameworks. Int J Refrig 2021;166: 506-518.
[108] Kabeel AE. Adsorption desorption operations of multilayer desiccant packed bed for dehumidification applications. (Dept. M), vol. 1. Mansoura University, Faculty of Engineering; 2020.
[109] Shuqing, et al. Metal-Organic Frameworks as advanced moisture sorbents for energy-efficient high temperature cooling. Scientific reports; 2018.
[110] Liu S, Jeong CH, Yeo MS. Effect of evaporator position on heat pump assisted solid desiccant cooling systems. Energies 2020;13.
[111] Avargani VM, Karimi R, Gheinani TT. Mathematical modeling of an integrated system for regeneration of solid desiccants using a solar parabolic dish concentrator. Int J Heat Mass Tran 2019;142(OCT). 118479.1-118479.14.
[112] Daghooghi-Mobarakeh H, Miner M, Wang L, Wang R, Phelan PE. Ultrasoundassisted regeneration of activated alumina/water adsorption pair for drying and dehumidification processes. Ultrasonics 2022;124:106769.
[113] Daghooghi-Mobarakeh H, Miner M, Wang L, Wang R, Phelan PE. Application of ultrasound in regeneration of silica gel for industrial gas drying processes. Dry Technol 2021:1–9.
[114] Jim´enez-Arreola M, Pili R, Dal Magro F, Wieland C, Rajoo S, Romagnoli A. Thermal power fluctuations in waste heat to power systems: an overview on the challenges and current solutions. Applied Thermal Engineering; 2018. S1359431117370710.
[115] Shanshan C, Wanyin H, Xu L, Xu L, Jiajun J. Experimental study on the impact factors of electro-osmotic flow in dehumidification applications. Energy Build 2020;202:109388. 109388.
[116] Nadra LAaR. Developed greener method based on MW implementation in manufacturing CNFs. Int J Nanomanufacturing 2019;15(3):269–89.
[117] Yang W, Wang W, Ding Z, Wang Z, Zhao X, He S. Performance study of a novel solar solid dehumidification/regeneration bed for use in buildings air conditioning systems. Energies 2017;10(9):1335.
[118] Ania CO, Parra JB, Men´endez JA, Pis JJ. Effect of microwave and conventional regeneration on the microporous and mesoporous network and on the adsorptive capacity of activated carbons. Microporous Mesoporous Mater 2005;85(1):7–15. 2005/10/23/.
[119] Motaghian S, Pasdarshahri H. Regeneration energy analysis and optimization in desiccant wheels using purge mechanism. J Build Eng 2020;27:100980. 2020/01/ 01/.
[120] Su M, Han X, Chang H, Chong D, Liu J, Yan J. Performance investigation and exergy analysis of a novel recirculated regenerative solid desiccant dehumidification system. J Build Eng 2023;67:106029. 2023/05/15/.
[121] Saputra DA, Osaka Y, Tsujiguchi T, Haruki M, Kumita M, Kodama A. Experimental investigation of desiccant wheel dehumidification control method for changes in regeneration heat input. Energy 2020;205.

[122] Bi Y, Yang W, Zhao X. Numerical investigation of a solar/waste energy driven sorption/desorption cycle employing a novel adsorbent bed. Energy 2018;149:84–97. 2018/04/15/.
[123] Sun XY, Dai YJ, Ge TS, Zhao Y, Wang RZ. Comparison of performance characteristics of desiccant coated air-water heat exchanger with conventional air-water heat exchanger – experimental and analytical investigation. Energy 2017;137:399–411. 2017/10/15/.
[124] Sun XY, Dai YJ, Ge TS, Zhao Y, Wang RZ. Heat and mass transfer comparisons of desiccant coated microchannel and fin-and-tube heat exchangers. Appl Therm Eng 2019;150:1159–67. 2019/03/05/.
[125] Venegas T, Qu M, Nawaz K, Wang L. Critical review and future prospects for desiccant coated heat exchangers: materials, design, and manufacturing. Renew Sustain Energy Rev 2021;151:111531. 2021/11/01/.
[126] Erkek TU, Gungor A, Fugmann H, Morgenstern A, Bongs C. Performance evaluation of a desiccant coated heat exchanger with two different desiccant materials. Appl Therm Eng 2018;143:701–10. 2018/10/01/.
[127] Amani M, Bahrami M. Greenhouse dehumidification by zeolite-based desiccant coated heat exchanger. Appl Therm Eng 2021;183:116178. 2021/01/25/.
[128] Ge TS, Cao W, Pan X, Dai YJ, Wang RZ. Experimental investigation on performance of desiccant coated heat exchanger and sensible heat exchanger operating in series. Int J Refrig 2017;83:88–98. 2017/11/01/.
[129] Ramzy A, AbdelMeguid H, ElAwady WM. A novel approach for enhancing the utilization of solid desiccants in packed bed via intercooling. Appl Therm Eng 2015;78:82–9. 2015/03/05/.
[130] Shamim JA, Hsu W-L, Kitaoka K, Paul S, Daiguji H. Design and performance evaluation of a multilayer fixed-bed binder-free desiccant dehumidifier for hybrid air-conditioning systems: Part I – experimental. Int J Heat Mass Tran 2018;116:1361–9. 2018/01/01/.
[131] Liang J-D, Hsu C-Y, Hung T-C, Chiang Y-C, Chen S-L. Geometrical parameters analysis of improved circulating inclined fluidized beds for general HVAC duct systems. Appl Energy 2018;230:784–93. 2018/11/15/.
[132] Bhabhor KK, Jani DB. Performance analysis of desiccant dehumidifier with different channel geometry using CFD. J Build Eng 2021;44:103021. 2021/12/01/.
[133] Liu M, Tu R, Chen X, Wu Z, Zhu J, Yang X. Performance analyses of an advanced heat pump driven fresh air handling system using active and passive desiccant wheels under various weather conditions. Int J Refrig 2022;141:1–11. 2022/09/01/.
[134] Tu R, Hwang Y. Efficient configurations for desiccant wheel cooling systems using different heat sources for regeneration. Int J Refrig 2017;86:14–27.
[135] Asadi A, Roshanzadeh B. Improving performance of two-stage desiccant cooling system by analyzing different regeneration configurations. J Build Eng 2019;25:100807. 2019/09/01/.
[136] Zhou X, Goldsworthy M, Sproul A. Performance investigation of an internally

cooled desiccant wheel. Appl Energy 2018;224(AUG.15):382–97.
[137] Zhou X, Reece R. Experimental investigation for a non-adiabatic desiccant wheel with a concentric structure at low regeneration temperatures. Energy Convers Manag 2019;201:112165. 2019/12/01/.
[138] Ge TS, Dai YJ, Wang RZ, Li Y. Experimental investigation on a one-rotor two-stage rotary desiccant cooling system. Energy 2008;33(12):1807–15.
[139] Jason, Woods. Membrane processes for heating, ventilation, and air conditioning. Renewable & Sustainable Energy Reviews; 2014.
[140] Abdullah S, et al. Technological development of evaporative cooling systems and its integration with air dehumidification processes: a review. Energy Build 2023; 283:112805. 2023/03/15/.
[141] Bui DT, Vivekh P, Islam MR, Chua KJ. Studying the characteristics and energy performance of a composite hollow membrane for air dehumidification. Appl Energy 2022;306:118161.
[142] Huang S-M, Yuan W-Z, Yang M. Advances in heat and mass transfer in the membrane-based dehumidifiers and liquid desiccant air dehumidification systems. Int J Heat Mass Tran 2019;139:881–906. 2019/08/01/.
[143] Niu R, Yang X, Kong X, Cui C, Li Y. A simulation study of the effects of membrane structure parameters on dehumidification performance of membrane-based liquid dehumidifier. J Build Eng 2023;78:107721. 2023/11/01/.
[144] Bai Z, et al. Performance evaluation of PVA/PEO/LiCl composite as coated heat exchangers desiccants. Int J Refrig 2023;154:258–67. 2023/10/01/.
[145] Gu C, Lv Y, Fan X, Zhao C, Dai C, Zhao G. Study on rheology and microstructure of phenolic resin cross-linked nonionic polyacrylamide (NPAM) gel for profile control and water shutoff treatments. J Petrol Sci Eng 2018;169:546–52. 2018/10/01/.
[146] Yao Y, Dai L, Jiang F, Liao W, Dong M, Yang X. Kinetic modeling of novel solid desiccant based on PVA-LiCl electrospun nanofibrous membrane. Polym Test 2017;64:183–93. 2017/12/01/.
[147] Li G-P, Qi R-h, Zhang L-Z. Performance study of a solar-assisted hollow-fibermembrane-based air humidification-dehumidification desalination system: effects of membrane properties. Chem Eng Sci 2019;206:164–79. 2019/10/12/.
[148] Chun L, Gong G, Fang X, Peng P, Li W. Investigation of dehumidification performance and flow characteristics of wavy vacuum membrane-based dehumidification modules. Chem Eng Res Des 2021;167:292–302. 2021/03/01/.
[149] Chun L, Gong G, Peng P, Li W, Fang X. Research on phase equilibrium effect and curve vacuum membrane-based dehumidification device. Int J Heat Mass Tran 2020;156:119879. 2020/08/01/.
[150] Zhao, et al. Simultaneous heat and water recovery from flue gas by membrane condensation: experimental investigation. Appl Therm Eng: Design, processes, equipment, economics 2017;113:843-850.
[151] Li C-H, Lin Z-J, Chang C-C, Rashidi S, Yan W-M. An experimental study on planar vacuum membrane dehumidifier equipped with serpentine flow channel plate. Alex Eng J 2023/02/01/2023;64:13–23.

[152] Liang C, Zeng Chung, Tai-Shung. Robust thin film composite PDMS/PAN hollow fiber membranes for water vapor removal from humid air and gases. Separation & Purification Technology; 2018.
[153] Scovazzo P, Scovazzo AJ. Isothermal dehumidification or gas drying using vacuum sweep dehumidification. Appl Therm Eng 2013;50(1):225–33.
[154] D. I. P. A. B, M. A. K. A, V. A. B. A, A. A. P. B, A. A. E. A. B, A. A. E. A. B. Membrane condenser heat exchanger for conditioning of humid gases. Sep Purif Technol 2023;241.
[155] Ahmadi M, Lindbrthen A, Hillestad M, Deng L. Subsea natural gas dehydration in a membrane contactor with turbulence promoter: an experimental and modeling study. Chem Eng J 2020:126535.
[156] V. V. U. A. C, V. V. T. A, A. Y. O. B, N. I. L. B. Membrane contactor air conditioning system: experience and prospects. Sep Purif Technol 2007;57(3):502–6.
[157] Liu L, Chen Y, K Y, Deng M. An industrial scale dehydration process for natural gas involving membranes. Chemical Engineering & Technology; 2001.
[158] Lin SW, Valera S. Air dehydration by permeation through dimethylpolysiloxane/ polysulfone membrane. Journal of the Mexican Chemical Society 2011;55:42–50.
[159] A DBJ, B MM, S. C PK. A critical review on application of solar energy as renewable regeneration heat source in solid desiccant – vapor compression hybrid cooling system - ScienceDirect. J Build Eng 2018;18(2018):107–24.
[160] Luo Y, Shao S, Xu H, Tian C, Yang H. Experimental and theoretical research of a fin-tube type internally-cooled liquid desiccant dehumidifier. Appl Energy 2014; 133(nov.15):127–34.
[161] Ge TS, Li Y, Wang RZ, Dai YJ. Experimental study on a two-stage rotary desiccant cooling system. Int J Refrig 2009;32(3):498–508. 2009/05/01/.
[162] A AK, B MA, C NAS, D VV, A MS. Experimental analysis of a solar assisted desiccant-based space heating and humidification system for cold and dry climates. Appl Therm Eng 2020;175.
[163] La D, Dai Y, Li H, Li Y, Kiplagat JK, Wang R. Experimental investigation and theoretical analysis of solar heating and humidification system with desiccant rotor. Energy Build 2011;43(5):1113–22.
[164] Niemann P, Schmitz G. Experimental investigation of a ground-coupled air conditioning system with desiccant assisted enthalpy recovery during winter mode. Appl Therm Eng 2019;160:114017.
[165] Mecenas P, Bastos RTDRM, Vallinoto ACR, Normando D. Effects of temperature and humidity on the spread of COVID-19: a systematic review. PLoS One 2020;15.
[166] Cai D, Qiu C, Zhang J, Liu Y, Liang X, He G. Performance analysis of a novel heat pump type air conditioner coupled with a liquid dehumidification/humidification cycle. Energy Convers Manag 2017;148(sep):1291–305.
[167] A HL, B SJL, A YS, B JWJ. Experimental study and prediction model of a liquid desiccant unit for humidification during the heating season. 2021.
[168] Su W, Zhang X. Performance analysis of a novel frost-free air-source heat pump with integrated membrane-based liquid desiccant dehumidification and humidification. Energy Build 2017;145(JUN):293–303.

[169] Koichi K, Wanghee C, Hitoshi K, Makoto K, Ryozo O, Shinsuke K. Field study on humidification performance of a desiccant air-conditioning system combined with a heat pump. Energies 2016;9(2):89.
[170] A RT, A JL, B YH. Fresh air humidification in winter using desiccant wheels for cold and dry climate regions: optimization study of humidification processes - ScienceDirect. Int J Refrig 2020;118:121–30.
[171] Kandeal AW, et al. Research progress on recent technologies of water harvesting from atmospheric air: a detailed review. Sustain Energy Technol Assessments Aug 2022;52. Art no. 102000.
[172] Rezaei, et al. Quantitative and qualitative characteristics of condensate water of home air-conditioning system in Iran. Desalination & Water Treatment Science & Engineering; 2015.
[173] Zolfagharkhani S, Zamen M, Shahmardan MM. Thermodynamic analysis and evaluation of a gas compression refrigeration cycle for fresh water production from atmospheric air. Energy Convers Manag 2018;170(AUG):97–107.
[174] Kumar M, Yadav A. Composite desiccant material “CaCl2/Vermiculite/Saw wood”: a new material for fresh water production from atmospheric air. Appl Water Sci 2016;7:2103-2111.
[175] Tu R, Hwang Y. Reviews of atmospheric water harvesting technologies. Energy 2020;201:117630.
[176] Kumar PM, Arunthathi S, Prasanth SJ, Aswin T, Babu PN. Investigation on a desiccant based solar water recuperator for generating water from atmospheric air. Mater Today Proc 2021;13.
[177] Gao Z, et al. Internally cooled membrane-based absorber for dehumidification and water heating: validated model and simulation study. Energy Convers Manag 2021;(Feb):230.
[178] Heidari A, Roshandel R, Vakiloroaya V. An innovative solar assisted desiccantbased evaporative cooling system for co-production of water and cooling in hot and humid climates. Energy Convers Manag 2019;185:396–409. 2019/04/01/.
[179] Tu R, Hwang Y. Performance analyses of a new system for water harvesting from moist air that combines multi-stage desiccant wheels and vapor compression cycles. Energy Convers Manag 2019;198:111811. 2019/10/15/.
[180] Tariq R, Sheikh NA, Xam´an J, Bassam A. An innovative air saturator for humidification-dehumidification desalination application. Appl Energy 2018;228: 789–807. 2018/10/15/.
[181] Wasti TZ, et al. An overview of solid and liquid materials for adsorption-based atmospheric water harvesting. Adv Mech Eng 2022;14(3):115–43.
[182] Park J-Y, et al. Empirical analysis of indoor air quality enhancement potential in a liquid-desiccant assisted air conditioning system. Build Environ 2017;121:11–25. 2017/08/15/.
[183] Guieysse B, Hort C, Platel V, Munoz R, Ondarts M, Revah S. Biological treatment of indoor air for VOC removal: potential and challenges. Biotechnol Adv 2008;26 (5):398–410. 2008/09/01/.
[184] Mahmood Z, Tian M, Field R. Membrane design for extractive membrane

bioreactor (EMBR): mass transport, developments, and deployment. J Membr Sci 2022;661:120948. 2022/11/05/.
[185] Fu H-X, Liu X-H. Review of the impact of liquid desiccant dehumidification on indoor air quality. Build Environ 2017;116:158–72. 2017/05/01/.
[186] Rong A, Liu M, Pang L, Yang D, Wang J, Zhou Y. Kinetics study of gas pollutant adsorption and thermal desorption on silica gel. Appl Sci 2017;7(6):609.
[187] Sheng Y, Fang L. Experimental analysis of the effect of moisture on air cleaning performance of desiccant wheel in a Clean Air Heat Pump. Build Environ 2019; 147:551–8.
[188] Yuxin P. Study on the performance of Metal-Organic Frameworks for indoor air purification and dehumidification. Master Master thesis. Beijing university of civil engineering and architecture; 2022.
[189] Xia H, Tang J, Aljerf L, Cui C, Gao B, Ukaogo PO. Dioxin emission modeling using feature selection and simplified DFR with residual error fitting for the grate-based MSWI process. Waste Manag 2023;168:256–71. 2023/08/01/.
[190] Tang J, Zhuang J, Aljerf L, Xia H, Wang T, Gao B. Numerical simulation modelling on whole municipal solid waste incineration process by coupling multiple software for the analysis of grate speed and air volume ratio. Process Saf Environ Protect 2023;176:506–27. 2023/08/01/.
[191] Sureshkannan V, Arjunan TV, Seenivasan D, Anbuudayasankar SP, Arulraj M. Parametric study on pressure-based packed bed adsorption system for air dehumidification. Proc IME E J Process Mech Eng 2021;235(5):1351–62.
[192] Liu Y, Chai JC, Cui X, Yan W, Li N, Jin L. Multi-objective optimization of air dehumidification membrane module based on response surface method and genetic algorithm. Energy Rep 2023;9:2201–12. 2023/12/01/.
[193] Liang C, Zeng S. Multi-objective design optimization of hollow fiber membranebased liquid desiccant module using particle swarm optimization algorithm. Heat Tran Eng 2018;39(17–18):1605–15. 2018/11/08.
[194] Ou X, Cai W, He X. Model-based optimization strategy for a liquid desiccant cooling and dehumidification system. Energy Build 2019;194:21–32. 2019/07/01/.
[195] Bhowmik M, Muthukumar P, Anandalakshmi R. Experimental based multiobjective optimisation for structured packed bed liquid desiccant dehumidification systems. J Build Eng 2020;32:101813. 2020/11/01/.
[196] Jiang Y, Wang X, Zhao H, Wang L, Yin X, Jia L. Dynamic modeling and economic model predictive control of a liquid desiccant air conditioning. Appl Energy 2020; 259:114174. 2020/02/01/.
[197] Zendehboudi A, Li X. Desiccant-wheel optimization via response surface methodology and multi-objective genetic algorithm. Energy Convers Manag 2018;174:649–60. 2018/10/15/.
[198] Zendehboudi A, Tatar A, Li X. A comparative study and prediction of the liquid desiccant dehumidifiers using intelligent models. Renew Energy 2017;114: 1023–35. 2017/12/01/.
[199] Wang X, Cai W, Yin X. A global optimized operation strategy for energy savings in

liquid desiccant air conditioning using self-adaptive differential evolutionary algorithm. Appl Energy 2017;187:410–23. 2017/02/01/.
[200] Demir MH, et al. Design of a proportional-control-based advanced control strategy for independent temperature and humidity control of a pre-cooled desiccant air cooling system. Appl Sci 2022;12(19):9745.
[201] Xu A, et al. Modeling and optimization of a solar-driven system coupled with liquid dehumidification and absorption refrigeration based on advanced exergy and exergoeconomic analyses. ACS Sustainable Chem Eng 2023;11(22): 8386–403. 2023/06/05.
[202] Liang C, Li X, Shi W, Wang B. A direct expansion air handling unit assisted by liquid desiccant for different sensible and latent heat ratios. Energy Build 2021; 238:110672. 2021/05/01/.
[203] Su W, Ma D, Lu Z, Jiang W, Wang F, Xiaosong Z. A novel absorption-based enclosed heat pump dryer with combining liquid desiccant dehumidification and mechanical vapor recompression: case study and performance evaluation. Case Stud Therm Eng 2022;35:102091. 2022/07/01/.
[204] Bassuoni MM. An experimental study of structured packing dehumidifier/ regenerator operating with liquid desiccant. Energy 2011;36(5):2628–38. 2011/ 05/01/.
[205] Kumar K, Singh A. Economic and experimental assessment of KCOOH hybrid liquid desiccant-vapor compression system. Sustainability 2022;14:15917.
[206] Li Y, Lu L, Yang H. Energy and economic performance analysis of an open cycle solar desiccant dehumidification air-conditioning system for application in Hong Kong. Sol Energy 2010;84(12):2085–95. 2010/12/01/.
[207] Ghali K, Othmani M, Ghaddar N. Energy consumption and feasibility study of a hybrid desiccant dehumidification air conditioning system in beirut. Int J Green Energy 2008;5(5):360–72. 2008/10/16.
[208] Luo J, Yang H. Energy, exergy, exergoeconomic and enviroeconomic (4E) assessment on a liquid desiccant air-conditioning system using green deep eutectic solvent of ethaline. Energy Convers Manag 2023;277:116685. 2023/02/ 01/.
[209] She X, Yin Y, Luo Y, Lindeman B, Zhong D, Zhang X. Experimental study of a novel subcooling method based on liquid desiccant dehumidification for vaporcompression refrigeration systems. Appl Therm Eng 2018;130:1460–71. 2018/ 02/05/.
[210] Guan Y, Zhang Y, Sheng Y, Kong X, Du S. Feasibility and economic analysis of solid desiccant wheel used for dehumidification and preheating in blast furnace: a case study of steel plant, Nanjing, China. Appl Therm Eng 2015;81:426–35. 2015/ 04/25/.
[211] Su B, Qu W, Han W, Jin H. Feasibility of a hybrid photovoltaic/thermal and liquid desiccant system for deep dehumidification. Energy Convers Manag 2018;163: 457–67. 2018/05/01/.
[212] Adedeji M, Abid M, Dagbasi M, Adun H, Adebayo V. Improvement of a liquid air energy storage system: investigation of performance analysis for novel ambient

air conditioning. J Energy Storage 2022;50:104294. 2022/06/01/.
[213] Keniar K, Ghali K, Ghaddar N. Study of solar regenerated membrane desiccant system to control humidity and decrease energy consumption in office spaces. Appl Energy 2015;138:121–32. 2015/01/15/.
[214] Ghaddar N, Ghali K, Najm A. Use of desiccant dehumidification to improve energy utilization in air-conditioning systems in Beirut. Int J Energy Res 2003;27 (15):1317–38.
[215] Liu Z, Cheng C, Han J, Zhao Z, Qi X. Experimental evaluation of the dehumidification performance of a metal organic framework desiccant wheel. Int J Refrig 2022;133:157–64. 2022/01/01/.
[216] Cui SQ, et al. Metal-Organic Frameworks as advanced moisture sorbents for energy-efficient high temperature cooling. Sci Rep Oct 2018;8. Art no. 15284.
[217] Chen Q, Cleland DJ, Carson JK, Walmsley TG. Integration of desiccant wheels and high-temperature heat pumps with milk spray dryers. Appl Therm Eng 2022;216: 119083. 2022/11/05/.
[218] Ma Y, Saha SC, Miller W, Guan L. Comparison of different solar-assisted air conditioning systems for Australian office buildings. Energies 2017;10(10):1463.
[219] Ding Z, et al. On-site measurement and simulation investigation on condensation dehumidification and desiccant dehumidification in Hong Kong. Energy Build 2022;254:111560. 2022/01/01/.
[220] Qi R, Lu L, Huang Y. Energy performance of solar-assisted liquid desiccant airconditioning system for commercial building in main climate zones. Energy Convers Manag 2014;88:749–57. 2014/12/01/.
[221] Abdel-Salam AH, Ge G, Simonson CJ. Thermo-economic performance of a solar membrane liquid desiccant air conditioning system. Sol Energy 2014;102:56–73. 2014/04/01/.
[222] Liang Y, Tang J, Xia H, Aljerf L, Gao B, Akele ML. Three-dimensional numerical modeling and analysis for the municipal solid-waste incineration of the grate furnace for particulate-matter generation. Sustainability 2023;15(16):12337.
[223] Kabeel Ae, Bassuoni MM. Feasibility study and life cycle assessment of two air dehumidification systems. 2013.
[224] Ortis A, Khatiwada D. A comparative life cycle assessment of two desiccant wheel dehumidifiers for industrial applications. Energy Convers Manag 2023;286: 117058. 2023/06/15/.